Master in Metabolism – Biopathology and Experimental

# Carbon dots as a potential therapy for breast cancer

Sofia Vanessa Mesquita Magalhães

Mentor: Professor Dr. Abel José Duarte, REQUIMTE/LAQV, ISEP, Polytechnic of Porto, Portugal; CIETI, ISEP, Polytechnic of Porto, Portugal

Co-Mentors: Dr. Hugo Fraga, FMUP, Faculty of Medicine of University of Porto, Portugal; i3S, instituto de Investigação e Inovação em Saúde, Portugal

Carla Luís, FMUP, Faculty of Medicine of University of Porto, Portugal; i3S, instituto de Investigação e Inovação em Saúde, Portugal

2023

*“The important thing is to never stop questioning.”*

**Albert Einstein**

# ACKNOWLEDGEMENTS

To the Biochemistry Department of the Faculty of Medicine of the University of Porto for making the place available to conduct my work.

To Professor Raquel Soares for her availability, understanding and help with the project.

To my mentor, Professor Dr. Abel Duarte, who accepted to be part of this adventure and for his support, dedication and learning. To my co-mentor Dr. Hugo Fraga for accepting to take part in this project. And to my co-mentor Carla Luís for all the support, affection, dedication and learning.

To all the colleagues in the department who took the time to help me and make some material available, especially Ilda Rodrigues, Susana Guerreiro, Carla Luís, André and Catarina.

To the International Iberian Nanotechnology Laboratory for generously providing the time and material to perform a technique necessary for this project.

And finally, to my parents and my best friends Ivo and Joana especially for their help, strength, support and for always being by my side.

# INDEX

Chapter 1 – Carbon Dots ..... 1
1.1 Synthesis ..... 3
1.2 Purification Processes ..... 5
1.3 Properties ..... 6
1.4 Functionalization ..... 7
1.5 Potential Therapy ..... 8
Chapter 2 – Breast Cancer ..... 10
2.1 Epidemiology ..... 10
2.2 Molecular Classification ..... 10
2.3 Detection and prognosis biomarkers in BC ..... 12
2.4 Risk Factors ..... 13
2.5 Detection ..... 14
2.6 Treatment ..... 16
Chapter 3 – Oxidative Stress ..... 18
3.1 ROS ..... 18
3.2 Antioxidant Mechanisms ..... 20
Chapter 4 – Aims ..... 21
Chapter 5 – Materials and Methods ..... 22
5.1 CD ..... 22
5.1.1 Synthesis ..... 22
5.1.2 Purification ..... 22
5.1.2.1.Dialysis ..... 22
5.1.2.2.Centrifugation/Filtration ..... 22
5.1.2.3.Lyophilization ..... 22
5.1.3 Characterization ..... 23
5.1.3.1.Homemade fluorometer ..... 23
5.1.3.2.Spectrophotometer ..... 23
5.1.3.3.Dynamic light scattering (DLS) ..... 23
5.1.3.4.Transmission Electron Microscopy (TEM) ..... 23
5.1.3.5.Fourier-transform infrared spectroscopy (FTIR) ..... 23
5.2 Cell culture ..... 24
5.2.1 MCF-10A and BT474 cell lines ..... 24
5.2.1.1.Cell culture ..... 24

5.2.1.2.Metabolic Activity Assay (MTT) ..... 24
5.2.1.3.BrdU Proliferation Assay ..... 24
5.2.1.4.Injury Assay ..... 24
5.2.1.5.Migration Assay ..... 25
5.2.1.6.Protein Extraction ..... 25
5.3 Oxidative Stress ..... 25
5.3.1 Antioxidant Enzymes ..... 25
5.3.1.1.SOD ..... 25
5.3.1.2.Catalase ..... 25
5.3.1.3.Total Glutathione (GSH) ..... 25
5.3.2 Antioxidant Activity ..... 26
5.3.2.1.DPPH ..... 26
5.4 Cytotoxicity Assay ..... 26
5.4.1 Intracellular Enzyme ..... 26
5.4.1.1.LDH ..... 26
5.5 Statistical Analysis ..... 26
Chapter 6 – Results ..... 27
6.1 CD ..... 27
6.1.1 Characterization ..... 27
6.1.1.1.Absorbance and fluorescence Spectrum ..... 27
6.1.1.2.DLS ..... 29
6.1.1.3.TEM ..... 29
6.1.1.4.FTIR ..... 30
6.2 Cell culture ..... 32
6.2.1 MCF-10A and BT474 cell lines ..... 32
6.2.1.1.Viability assay ..... 32
6.2.1.2.Proliferation Assay ..... 33
6.2.1.3.Injury ..... 33
6.2.1.4.Migration ..... 34
6.3 Oxidative Stress ..... 36
6.3.1 Antioxidant Enzymes ..... 36
6.3.1.1.SOD ..... 36
6.3.1.2.Catalase ..... 36
6.3.1.3.GSH ..... 37

6.3.2 Antioxidant Activity ..... 38
6.3.2.1.DPPH ..... 38
6.4 Cytotoxicity Assay ..... 39
6.4.1 Intracellular Enzyme ..... 39
6.4.1.1.LDH ..... 39
Chapter 7 – Discussion ..... 41
Chapter 8 – Conclusion ..... 46
Chapter 9 – Future Perspectives ..... 47
Chapter 10 – References ..... 48

# FIGURE INDEX

Figure 1 - Types of CD (A)[13] according to surface groups, properties and core structure and the different CD applied in biomedicine (B)[12]. ..... 3
Figure 2 - Scheme of the demonstration of CD synthesis according to top-down and bottom-up methods. ..... 4
Figure 3 - Estimated number of new cancer cases (A) and deaths (B) in 2020 in the world for the female population. ..... 10
Figure 4 - Schematic representation of the molecular subtypes of BC. ..... 11
Figure 5 - Schematic diagram representing the purification processes of CD. ..... 23
Figure 6 - Absorbance (A) and fluorescence (B) spectrum of CD. ..... 27
Figure 7 - Absorbance and fluorescence spectra of CD after dialysis (CD_D) (A and B) and DEG diluted in deionized water (C and D). The same concentration of CD and DEG was used so that we could compare by fluorescence. ..... 28
Figure 8 - Graphical representation of CD purification steps. This schematic represents the dialysis (CD_D), after centrifugation (CD_DC) and 0,22 μm filter (CD_DCF) as well as the pellet (CD_DCF-P) and the use of the 3 kDa molecular filter (CD_DCF3) and the pellet (CD_DCF3-P). 28
Figure 9 - CD hydrodynamic diameter (A) and zeta potential (B). ..... 29
Figure 10 - TEM images demonstrating the size and round morphology of the CD (A and B) and high-resolution transmission electron microscopy images where their crystalline structure is visualized (C). CD were highlighted with orange arrows. ..... 30
Figure 11 - FTIR spectrum of the CD. Each absorption peak represents vibrations in a functional group, in this case characteristic CD functional groups: O-H, O-H, C=C, C-H, O-H, C-O, C-O, O-H, C=O, respectively. ..... 31
Figure 12 - Cell viability assay of MCF-10A at different concentrations of CD. Values are statistically significant compared to the control (C), except for 1 mg/mL. ***p-value < 0.001; ****p-value < 0.0001. ..... 32
Figure 13 - Cell viability assay of BT474 cells at different concentrations of CD. Values are statistically significant compared to the control (C). *p-value < 0.05; ***p-value < 0.001; ****p-value < 0.0001. ..... 32
Figure 14 - Cell proliferation assay of MCF-10A (A) and BT474 (B) cells measured at CD concentrations close to IC50. Values are statistically significant compared to control (C). ***p-value < 0.001; ****p-value < 0.0001. ..... 33
Figure 15 - Representation of the injury assay at T0 and T24. The injury assay of MCF-10A cells was performed with CD at concentrations near the IC50. ..... 33
Figure 16 - Representation of the injury assay at T0 and T24. The injury assay of BT474 cells was performed with CD at concentrations near the IC50. ..... 34
Figure 17 - Injury assay of MCF-10A (A) and BT474 (B) cells measured at CD concentrations close to the IC50. The values are not statistically significant compared to the control (C). ..... 34
Figure 18 - Cell migration of MCF-10A (A) and BT474 (B) measured at CD concentrations close to IC50. Values are statistically significant compared to control (C), except for 6 mg/mL in MCF-10A. **p-value < 0.01; ****p-value < 0.0001. ..... 35
Figure 19 - Percentage of SOD inhibition in MCF-10A (A) and BT474 (B) cell lines measured at CD concentrations close to IC50. The values are not statistically significant compared to the control (C). ..... 36

Figure 20 - Catalase activity (mU/mL) in MCF-10A (A) and BT474 (B) cell lines measured at CD concentrations close to IC50. The values are not statistically significant compared to the control (C). ..... 37
Figure 21 - GSH (µM) in MCF-10A (A) and BT474 (B) cell lines measured at CD concentrations close to the IC50. The values are not statistically significant compared to the control (C)..... 37
Figure 22 - DPPH activity (TEq) in MCF-10A (A) and BT474 (B) cell lines measured at CD concentrations close to the IC50. The values are statistically significant compared to the control (C). *p-value < 0.05; **p-value < 0.01; ****p-value < 0.0001..... 38
Figure 23 - DPPH activity (TEq) in CD diluted in MCF-10A (A) and BT474 (B) culture medium and water (C) at concentrations close to the IC50. The values are not statistically significant compared to the control (C)..... 39
Figure 24 - Total LDH (U/L) in MCF-10A (A) and BT474 (B) cell lines measured at CD concentrations close to IC50. The values are not statistically significant compared to the control (C). ..... 40

# ABBREVIATIONS

| | |
|---|---|
| **BC** | Breast Cancer |
| **CD** | Carbon Nanoparticles |
| **CD_D** | CD after Dialysis |
| **CD_DC** | Dialyzed CD after Centrifugation |
| **CD_DCF** | Dialyzed CD after Centrifugation and use of 0,22 μm Filter |
| **CD_DCF-P** | Pellet of dialyzed CD after Centrifugation and use of 0,22 μm Filter |
| **CD_DCF3** | Dialyzed CD after Centrifugation and use of 0,22 μm Filter and 3 kDa molecular filter |
| **CD_DCF3-P** | Pellet of dialyzed CD after Centrifugation and use of 0,22 μm Filter and 3 kDa molecular filter |
| **DEG** | Polyethylene glycol |
| **DPPH** | 2,2-Diphenyl-1-picrylhydrazyl |
| **GSH** | Total Glutathione |
| **HER2/neu** | Human Epidermal Growth Factor Receptor 2 |
| **LDH** | Lactate Dehydrogenase |
| **PR** | Progesterone Receptor |
| **ROS** | Reactive Species of Oxygen |
| **SOD** | Superoxide Dismutase |
| **TEM** | Transmission Electron Microscopy |

# Resumo

As nanopartículas de carbono (CD) são nanomateriais fluorescentes à base de carbono que têm sido alvo de investigação desde 2004[1]. As CD são caracterizadas de acordo com o seu tamanho compreendido entre 2 e 100 nm e pela presença à superfície de grupos polares de carbonilo e carboxilo[1]. Das vantagens destacam-se a fotoluminescência e as suas propriedades químicas e físicas[1]. A sua manipulação é realizada pelas técnicas de síntese através da decomposição de material orgânico denominada top-down ou do crescimento e aglomeração de átomos e moléculas designada bottom-up[1]. Após síntese, os grupos à superfície possibilitam a funcionalização com diversos compostos[1]. O sucesso destas aplicações depende da composição química superficial das CD[1]. Estas estruturas nanométricas possuem boa biocompatibilidade e reduzida toxicidade o que permite uma boa interação com sistemas biológicos[1]. Estas propriedades permitiram que as CD fossem introduzidas como potencial terapêutico no cancro, nomeadamente no cancro da mama, associadas a sistemas de transporte de fármacos, bioimagem, biossensor, terapia microbial, fototermal e fotodinâmica[2]. O cancro da mama (BC) é o cancro mais prevalente e com maior taxa de mortalidade na população feminina em todo o mundo[3].

Neste estudo, testamos a utilização de CD derivadas de frutose para terapia antitumoral de cancro da mama. De acordo com a revisão da literatura realizada, estes são os primeiros ensaios efetuados utilizando a frutose como fonte de carbono para a síntese de nanopartículas. Sendo estas sintetizadas por irradiação micro-ondas pelo método bottom-up. Depois de purificadas, as CD foram caracterizadas em função da sua morfologia, tamanho, estrutura, fluorescência e grupos funcionais com recurso a microscopia eletrónica de transmissão (TEM), dispersão dinâmica de luz (DLS), espectrofotómetro de fluorescência e espectroscopia de infravermelho com transformada de Fourier (FTIR), respetivamente. Como expectável, as CD derivadas de frutose são compostas por carbono, oxigénio e hidrogénio. Como também é característico das CD, são fluorescentes com um espectro de absorção de 360 nm e um espectro de emissão com uma banda de emissão larga (cerca de 520 nm). Apresentam morfologia redonda com tamanhos entre 2 e 6 nm (tamanho média das partículas de 3.1 ± 1.8 nm), diâmetro hidrodinâmico inferior a 2 nm e estrutura cristalina.

Em ensaios de cultura celulares de células tumorais e não tumorais, as CD exibiram maior citotoxicidade e menor proliferação celular nas células tumorais de mama em comparação com as células epiteliais mamárias. Apesar de existir alguma toxicidade ao nível das células epiteliais. Em adição, as CD afetaram mais a migração celular e o dano celular das células tumorais da mama.

Em relação à atividade das principais enzimas associadas a stress oxidativo, os resultados revelaram que as enzimas antioxidantes superóxido de dismutase (SOD) e catalase exibiram menor atividade nas células tumorais enquanto a glutationa total (GSH) exibiu maior atividade exceto em 6 mg/mL. A enzima intracelular lactato desidrogenase (LDH) total libertada para o meio extracelular é menor nas células tumorais exceto no controlo. E o poder antioxidante medido a partir do DPPH é maior nas células tumorais.

**Palavras-chave:** Nanopartículas de carbono; cancro da mama; cultura de células; metabolismo tumoral

# Abstract

Carbon nanoparticles (CD) are fluorescent carbon-based nanomaterials and have been the subject of research since 2004[1]. CD are characterized by their size between 2 and 100 nm and by the presence of polar carbonyl and carboxyl groups on their surface[1]. The major advantages of CD are their photoluminescence and their chemical and physical properties[1]. Nanoparticle formation is accomplished by synthesis techniques through the decomposition of organic material called top-down or the growth and agglomeration of atoms and molecules called bottom-up[1]. After synthesis, the surface groups enable the functionalization with various compounds[1]. The success of these applications depends on the surface chemical composition[1]. These nanostructures have good biocompatibility and low toxicity, which allows good interaction with biological systems[1]. These properties have allowed CD to be introduced as potential therapeutics in cancer, namely in breast cancer associated with drug transport systems, bioimaging, biosensor, microbial, photothermal and photodynamic therapy[2]. Breast cancer (BC) is the most prevalent cancer with the highest mortality rate in the female population worldwide[3].

In this study, we tested the use of fructose-derived CD for antitumor therapy of breast cancer. According to the performed literature review, this is the first assays using fructose as a carbon source for the synthesis of nanoparticles. These were synthesized by microwave irradiation by bottom-up method. After purification, CD were characterized for their morphology, size, structure, fluorescence and functional groups with resource to transmission electron microscopy (TEM), dynamic light scattering (DLS), fluorescence spectrophotometer and Fourier transform infrared spectroscopy (FTIR), respectively. As expected, fructose-derived CD were composed of carbon, oxygen and hydrogen. As is also characteristic of CD, they were fluorescent with an absorption spectrum at 360 nm and an emission spectrum with a broad emission band (around 520 nm). They had a round morphology with sizes between 2 and 6 nm (average particle size 3.1 ± 1.8 nm), a hydrodynamic diameter of less than 2 nm and a crystalline structure.

Regarding cell-based assays with breast cancer and breast epithelial cell lines, CD exhibited higher cytotoxicity and lower cell proliferation in breast tumor cells compared to breast epithelial cells. Nonetheless, there was some toxicity at the epithelial cell level. Furthermore, cell migration and injury were more profoundly affected in breast tumor cells.

Regarding the activity of the main enzymes associated with oxidative stress, the results revealed that the antioxidant enzymes superoxide dismutase (SOD) and catalase exhibited lower activity in tumor cells while total glutathione (GSH) exhibited higher activity except at 6 mg/mL. Total intracellular enzyme lactate dehydrogenase (LDH) released into the extracellular environment is lower in tumor cells except in the control. And the antioxidant power measured by 2,2-Diphenyl-1-picrylhydrazyl (DPPH) is higher in tumor cells.

**Keywords:** Carbon nanoparticles; breast cancer; cell culture; tumor metabolism

# Chapter 1 – Carbon Dots

Carbon nanoparticles (CD) are fluorescent carbon-based nanomaterials characterized by their nanosize between 2 and 100 nm and the presence of polar carbonyl and carboxyl groups on their surface[1]. Research on CD goes back to 2004 while preparing carbon nanotubes through the electrical collapse of a gas[1,4]. This finding was a significant breakthrough in biomedicine due to their exceptional properties, including its fluorescence, good biocompatibility, low cytotoxicity[4] and the ability to incorporate into biological systems as anticancer agents, sensors and light emitters. Additionally, synthesis from green organic matter allows for large-scale, low-cost production and reuse[5]. These CD are also easily functionalized with other compounds due to their functional groups[6]. Either with atoms as nitrogen, sulfur, phosphorus and boron or with metal atoms like zinc, terbium, gadolinium, copper, germanium, cobalt and magnesium[6]. In addition, there are already studies showing functionalization with drugs used in breast cancer treatments such as doxorubicin[7].

Nanoparticles are a heterogenous class of carbon structures that can be characterized based on their surface groups, properties and core structure as show in **figure 1**. These categories include nanoparticles as CD, carbon quantum dots, graphene quantum dots and carbonized polymer dots[8–10].

- CD have high carbonizing power but an irregular structure, with presence of chemical groups on the surface[10].
- Carbon quantum dots are spherically shaped nanoparticles with a regular and perfect structure and chemical groups on the surface[10]. They usually have a semiconductor core and a capsule that contains a large band gap in the fluorescence spectrum[4].
- Graphene quantum dots are single or diverse sheet structures composed of graphene with chemical groups present in the vicinity of or between the graphene sheets[10]. Their structure is usually regular, with the same number of layers and the same size[10].
- Carbon polymer dots have a heterogeneous structure (polymer/carbon) composed of functional groups and polymer chains[10]. Their carbon core can be divided into 4 subclasses: 2 completely carbonized cores, a paracrystalline structure with surrounding carbon clusters, dehydrated and cross-linked bonds between polymer chains and closed-loop covalent bonds[10].

Nanoparticles applied to biomedicine are based on liposomes, polymers, polymer micelles, dendrimers, solid lipids and nanostructured lipid transporters and inorganic nanoparticles as gold and mesoporous silica nanoparticles.

- In nanoparticles-based liposomes, PEGylation (modifications in biological molecules from covalent or non-covalent bonds with polyethylene glycol)[11] on the surface allows higher half-life which in turn improves the therapeutic effect. Liposomes vary in size and can contain one or more double layers, so there is the possibility of incorporating hydrophilic drugs into the water-containing core and hydrophobic ones into the lipid layer[12].
- Nanoparticles based-polymers are made from bio-composite material that is compatible with biological systems and are able to functionalize with chemotherapeutic drugs by

encapsulation or conjugation. With functionalization, these nanoparticles can be more effective in the drug release system and improving its effect[12].

- Nanoparticles based-polymer micelles are nanotransporters with a hydrophobic core and a hydrophilic surface. These can increase their ability to invade the tumor vascular system, making them effective drug transporters. The core has the ability to incorporate hydrophobic drugs and in addition, they typically transport drugs with a low ability to dissolve in water[12].
- Nanoparticles based-dendrimers consist of a core, successive branched parts and a no specific functional group on the outer surface. Since their core is hydrophobic, they have the ability to improve the solubility of hydrophobic drugs. Drug dose and directionality can be optimized through alterations on the branched parts. The functional group can be functionalized or chemically altered to function as an imaging intermediate, as well. These share the same feature of the other described nanoparticles, as a promising deliver system for chemotherapeutical[12].
- Nanoparticles based-solid lipids have a solid lipid base composed primarily of fatty acids, wax and fatty acid esters. They are characterized by their solidification at room and body temperature. The drug is delivered either by binding to the lipid surface or by penetration into the core. They are commonly used to improve the bioavailability of drugs with reduced water solubility. In addition, they are easily produced, can contain higher doses of drug with limitations and are effective in their release and stability[12].
- Nanoparticles based-nanostructured lipid transporters were developed to fight the obstacles of nanoparticles based-solid lipid and their limitations. Such limitations include drug quantity, crystal formation when there is drug leakage and the appearance of polymorphic transitions[12]. These nanoparticles consist of both solid and liquid lipids, their matrix is non-structured and remains in the solid state either at room or body temperature. When in the liquid state it facilitates the dissolution of the drug and payload.
- Gold nanoparticles have been a major development due to their properties such as biocompatibility, photothermal therapy agents, contrast in imaging, multifunctional and easy functionalization[12].
- Nanoparticles silica mesoporous are drug delivery carriers since they are characteristic for their ease of pore size modification, large storage capacity, multifunctional, no early drug release and pharmacokinetic properties[12].

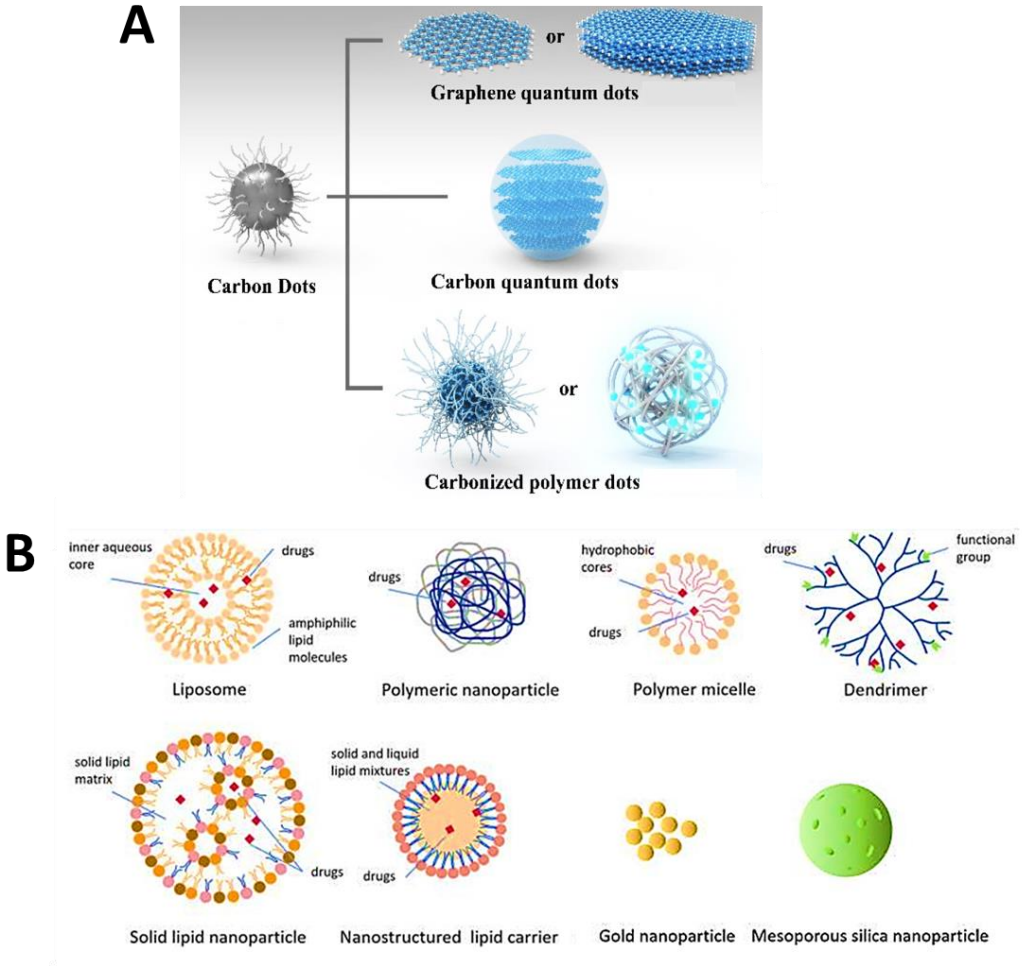


*Figure 1 - Types of CD (A)*[13] *according to surface groups, properties and core structure and the different CD applied in biomedicine (B)*[12].

The different synthesis methods form CD with different properties such as their fluorescence and size[1]. The size of these nanostructures can be altered in the synthesis process by modifications in the reaction time, temperature and solvent[1].

## 1.1 Synthesis

CD properties highly depend on external factors such as temperature, reaction time and solvent[8]. Although sugars are the primary source of carbon for CD formation, green organic matter such as lemon peel, banana peel and juice, tender coconut and eggshell can also be used with advantages such as low energy consumption, ease of access and reuse of organic matter[14].

CD can be produced using two synthesis techniques, namely top-down and bottom-up, as shown in **figure 2**[1,8]. Top-down technique involves the decomposition of organic material using various methods such as laser ablation, arc discharge, electrochemical and chemical oxidation, electrolysis, ultrasonic passivation and acid etching[1,8,15]. This method requires complex equipment and strong reagents with low efficiency rate[8]. Also, carbon sources are limited and the preparation of CD can lead to the formation of unique chemical groups on their surface, making it difficult to control their properties[8].

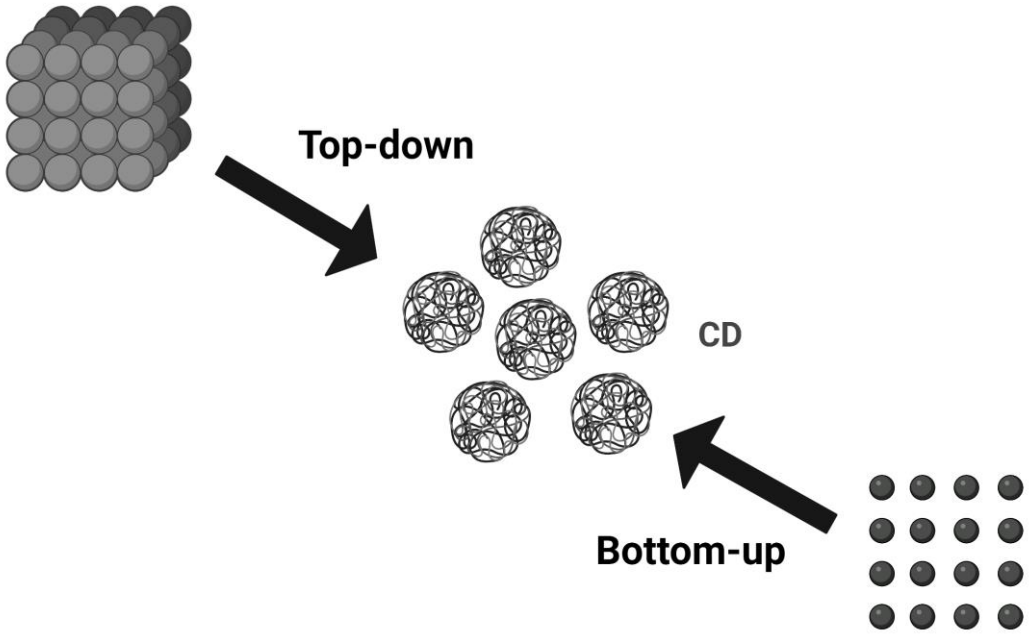


*Figure 2 - Scheme of the demonstration of CD synthesis according to top-down and bottom-up methods.*

Arc discharge involves using carbon electrodes heated to high temperatures by means of an electric current, in the absence of oxygen. While it is simple to perform, the costs are high compared to laser ablation and microwaves[16].

Laser ablation employs a laser as an energy source that leads to the vaporization of the carbon source. The vapor obtained is collected in a copper collector that is cooled with water and the vapor then passes through a neutral gas stream and condenses. This technique is suitable for controlling particle size but requires a significant investment[16].

Chemical oxidation uses an oven as the energy source containing either an infrared resistor, a lamp, or a hot filament that decomposes a precursor gas and heats the sample. It is easy to perform and enables the production of nanoparticles, homogeneous in size[16].

Electrochemical oxidation is carried out through a process called ionic liquid-dependent chemical exfoliation in which anodic oxidation of water and anionic intercalation of the ionic liquid used lead to the formation of CD[16]. The resulting nanoparticles have high purity and yield, but the process is complex[16]. This approach is a method by which carbons are separated from a graphite rod immersed in a mixture containing an anionic fluid and anodized water[17]. The separation occurs through the interaction of the compounds in the mixture and the CD can be removed through centrifugation[17].

In ultrasonic passivation, carbon samples are subjected to oxidizing and high-wave ultrasonic conditions, leading to the breakdown of carbon and the formation of CD[17].

On the other hand, the bottom-up technique involves the growth and agglomeration of atoms and molecules through various reactions such as hydrothermal and solvothermal reactions, pyrolysis, solvent-free methods, microwave irradiation techniques or plasma treatment[1,8,16].

In the formation of CD using this method, molecules commonly go through four stages: condensation, polymerization, carbonization and passivation[18]. During condensation, intermediate chain compounds are formed from organic molecules[18]. Polymerization occurs in these intermediate chain compounds, leading to the formation of polymers with covalent or non-covalent connections[18]. Carbonization involves the formation of a carbon core, especially at high temperatures[18]. Finally, passivation is performed to enhance luminescence performance[15]. This mechanism is highly favored for green synthesis, as organic substances can be transformed into CD through the carbonization of small organic molecules[19]. This method offers several advantages such as the availability of various carbon sources for CD formation, ease to manipulate and easy to control their properties. Adjusting temperature, pressure, time and solvent with the use of simple and inexpensive equipment allows the manipulation of the CD properties.

CD synthesized from hydrothermal reactions have a greater ability to functionalize with other substances compared to other techniques. The hydrothermal technique involves a control system of temperature and pressure in an aqueous or mineralized medium that allows material dissolution insoluble under normal conditions. Through this method, size, shape, surface modification and stability of CD can be precisely controlled. It is the most used technique due to its low cost, low temperature requirement and eco-friendliness[17].

The solvothermal reaction technique is similar to hydrothermal, but uses organic solvents instead, resulting in nanoparticles with low yield, purity and homogeneity in particle size. Microwave synthesis offers several advantages such as ease production, high speed, low cost and energy efficiency. It transforms electromagnetic energy into thermal energy, allowing for the formation of nanoparticles with high yield and purity[17].

Plasma treatment involves two components: microwave plasma with nitrogen radicals in thermodynamic equilibrium and plasma with pure nitrogen. The plasma flame is formed by microwave radiation. Gas injection enables gas stirring of the plasma flame, allowing carbon atoms to mix with iron atoms produced by the plasma flame, resulting in the development of carbon nanomaterials[16].

Microwave irradiation is an easy-to-use technique with a fast reaction time and low costs. The microwave provides an energy source as a homogeneous heat source for the CD formation process, resulting in particles that are usually uniform in size. This technique also allows the particle size to be controlled by the reaction time. Because of all its potential, the CD in this study were synthesized using this method[16].

## 1.2 Purification Processes

The main objective of purification is to eliminate impurities from the CD, thus increasing their purity and also homogenize their size. They provide the quality control necessary for the use of these CD in biological systems. Electrophoresis, centrifugation, dialysis and column chromatography are common methods used to purify CD[20].

Electrophoresis is a method of separating particles according to their charge and/or mass. This is an effective process with good purification rates[18].

In centrifugation, nanoparticles are separated according to their density through high-speed rotation[21]. This results in the elimination of impurities that CD may contain[20]. In conjunction with ultracentrifugation, it is possible to separate carbon points from the solution[20]. Centrifugation can also be used with filtration through a 0,22 µm filter[22].

Another purification process is dialysis. This process separates biomolecules through use of a sleeve containing a porous semi-permeable membrane with desired size. The sleeve contains the solute and is immersed in a solvent, usually water. This creates a solute/solvent gradient which leads to separation of particles by diffusion due to the imbalance in the system. Particles larger than the pore diameter of the sleeve membrane remain inside and smaller particles migrate to the outside of the sleeve. This process is easy to use, has low energy consumption and high separation efficiency[20,23].

Lastly, chromatography is a technique based in the passage of the sample through a column containing a solid phase, usually silica. The liquid sample is inserted into the column surface and moves according to its affinity and interactions with the column. This allows the particles to exit the column at different times, separating them according to their size. However, it has disadvantages such as difficult handling and high purity carbon points in a short time, continuous separation and poor efficiency[20].

To achieve better results, i.e., higher purity, it is sometimes necessary to combine several processes[20].

## 1.3 Properties

CD have common characteristics such as low toxicity, sustainability, stability, fluorescence, quantum size effect, thermal stability and chemical inertness[16,24].

Photoluminescence is a defining characteristic of CD and their ability to emit light at various wavelengths makes them suitable for applications such as bioimaging[24]. Although most CD emit blue or green light, there are different routes and precursors for the synthesis of nanoparticles[24]. In addition, they also exhibit fluorescence stability, pH sensitivity and photobleaching resistance[25] that can be caused in CD synthesis by the factors of reaction time and temperature[26].

Absorption is also a feature of CD. Absorption spectrum changes depending on the carbon source and the synthesis method. Absorption peaks between 350 and 600 nm mean that topic chemical groups may contribute to the absorption in the UV-Vis region. In certain CD, the absorption spectrum shows deviations, meaning differences in the structure or composition of the distinct hybridization derivatives[25].

Photoinduced electron transfer has been one of the most investigated properties, especially in the conversion of light into energy. CD also have photocatalytic properties that allow them to be incorporated into photocatalytic systems in order to enhance catalysts[25].

CD must be biocompatible and non-toxic to biological systems so that they can be tested without affecting the system[16]. These unique properties allow their use in bioimaging and nano-transport alongside with compound delivery systems[1].

## 1.4 Functionalization

Functionalization of CD is a major advantage that enables the development of sensors and the amelioration of the aggressive side effects caused by drugs used in chemotherapy[6]. It also enhances the properties of CD, improves biocompatibility[22] and allows them to be targeted to specific locations[6]. There are two main methods of functionalization - doping and surface functionalization[6]. These techniques which include encapsulation and molecularly imprinted polymers allows the improvement of drug transport by directing to a specific target[22].

Doping involves internalizing atoms like nitrogen, sulfur, phosphorus and boron on the surface of CD, which improves their optical and photoluminescent properties[6]. Metal atoms like zinc, terbium, gadolinium, copper, germanium, cobalt and magnesium can also be used to incorporate new functionalities[6]. Doping with nitrogen has several advantages such as increased fluorescence quantum yield, lower cytotoxicity and improved fluorescence performance[27]. Adding graphite to nitrogen can result in a redshift of energy altering the absorption spectra[27]. Doping with non-metals leads to increased fluorescence through composition and structure alterations or by the formation of polyaromatic structures that compose new structure states[27].

Surface functionalization, on the other hand, consists in the addition of polymers and organic and inorganic molecules to the surface of CD[6]. This method improves their photochemical, photophysical, photoluminescent and drug-delivery properties and is commonly used in biomedicine[6,16]. Covalent bonding between quinoline and CD allows capture of zinc ions, which provides dual fluorescence assessed from magnetic resonance imaging; amino and carbon disulfide groups activate fluorescence in the presence of $Hg^{2+}$; BHHCT-$Eu^{3+}$ complex can detect Cu2+ radiometrically; atom transfer radical polymerization (ATRP) has developed a robust sensor for gene delivery and bioimaging[28].

CD functional groups with oxygen facilitates the process due to their negative charge and polarization. This provides a better interaction with the compound by its physical and chemical stability. Small molecules, peptides, aptamers and antibodies that bind to CD for targeting purposes, act as drug transporters, bioimaging agents and sensors. One example is folic acid that is able to be conjugated to detect tumor cells since it has affinity for the folate receptor that is highly expressed in certain tumor cells. Transferrin targets various tumor cells such as lung, brain, breast and colorectal cancer since there is an overexpression of its receptors in the cell membrane of tumor cells. Arginine, glycine and aspartic acid are used for tumor cell detection. Mannose can be used as a marker for bacteria[22,29].

Different approaches such as covalent bonds, hydrogen bonds and electrostatic interactions can be used for surface functionalization[6]. Covalent bonds are particularly strong and are used in biomolecules catalysts like ethyl carbodiimide and N-hydroxysuccinimide[6]. This method allows the capture of zinc ions, activation of fluorescence in the presence of $Hg^{2+}$, radiometric detection of $Cu^{2+}$ and development of a robust sensor for gene delivery and bioimaging using atom transfer radical polymerization[6]. Overall, functionalization of CD enhances their optical properties and their applications in biomedicine, including bioimaging and radiotherapy[6]. This

type of functionalization shows higher fluorescence emission because the surface defect is more stable, facilitating the ability of radioactive recombination of electron capture on the surface[30].

Encapsulation is mostly used in drug delivery where it protects the drug from being eliminated or released before it reaches its destination. Typically, the capsule is made up of matrices of gel or polymeric nanostructures that trap the target drug[22].

Molecularly imprinted polymers are a technique to create synthetic polymers able to recognize molecules and function as a detection receptor. Synthetization is accomplished by polymerizing monomers with a target analyte. Afterwards, the analyte is removed, leaving a gap about its size. This space will allow binding with other target analytes with identical structure. The CD incorporated with this technique, can convert the binding activity into visible optical properties. There are other approaches to these identifiers such as nonimprinted polymer synthesis and the use of amino-CDs (functional monomer) and mesoporous silica (matrix) where there is increased sensitivity for detection[22].

Polyphenols, which are already considered natural antioxidants from fruits, vegetables, tea, oils and cereals, can be functionalized with CD. This makes it possible to improve their biocompatibility, water solubility and increase their antioxidant and anti-inflammatory power. Some examples of polyphenols used in BC are quercetin, curcumin and resveratrol. Studies have shown that gold nanoparticles as a carrier for the polyphenol quercetin decreased tumor size as well as increasing the expression of genes associated with cell apoptosis; resveratrol in conjunction with albumin nanoparticles decreased tumor volume and necrotic tissue was treated with reduced side effects; chitosan-coated liposomes with curcumin decreased tumor growth and increased the antitumor effect[31,32].

The use of biomass from plants in conjunction with CD has played an important role in the diagnosis and treatment of cancer. Some plants exhibit antitumor characteristics and induce cellular cytotoxicity and apoptosis. Functionalized with CD have photostability, photoluminescence, water solubility and show no cytotoxicity. The use of ginger juice and green tea in combination with CD led to inhibition of breast cancer cell growth. Ginseng-derived CD exhibit antioxidant and anti-inflammatory activity in cancer[33].

## 1.5 Potential Therapy

Recently, CD have been explored as a promising option in drug delivery systems to target specific substances for the cancer treatment[2]. Anti-tumor strategies using CD (or nanoparticles) can include passive, active and stimulus response[12].

Passive targeting is associated with the ability of nanoparticles to accumulate in tumor tissues due to increased permeability and retention effect. It is known that tumor cells, in hypoxic situations, release factors such as HIF1 which promotes angiogenesis, the formation of new vessels. Also, lymphatic function is disrupted, so there is little absorption of interstitial fluid which allows for greater retention of CD in tumor cells. These conditions are the key to greater selective accumulation of chemotherapy drugs against BC. However, tumors have heterogeneous individual characteristics, so this type of strategy is difficult to combat BC. In active targeting, is important to identify ligands for target receptors. With this, nanoparticles functionalized with these target receptors, can increase their ability to deliver drugs into tumor

tissue. The ligands depend on the overexpression of the target that differs in each type of cancer. Finally, targeting by response to internal (changes at the level of redox potential, pH and enzymes) or external (temperature, pressure, photodynamic therapy, ultrasound and electric field) stimuli. These stimuli will lead to a selective release of drugs into tumor tissues and avoid toxicity in the system[12].

Due to their nano size, CD can cross cell membranes, allowing for controlled release of drugs at the desired location with a longer duration in the circulatory system[2]. This precise targeting approach minimizes damage to healthy cells, making it an effective strategy for cancer treatment[2]. Furthermore, CD can be functionalized to cross the blood-brain barrier, detect cellular components associated with degenerative diseases and remove superoxide radicals associated with the central nervous system[6,16].

CD have also shown potential in bioimaging and biosensor applications as previously described. They can be functionalized to detect various molecules, such as ions, cations, metals and bioactive molecules, making them useful in chemical sensing and gene therapy. CD functionalized with polyethylenimine, hyaluronic acid and chitosan have demonstrated effectiveness as gene transporters[6,16].

Interaction with metal ions by energy transfer, results in electron-hole recombination and particularize CD as chemical detectors[34]. CD have also been studied in microbial therapy, showing antiviral effects and enhancing the passage of compounds through bacterial membranes[16].

In cancer therapy, CD can be used in photodynamic and photothermal therapy to destroy tumor cells using laser light, usually, near infrared radiations[6,34]. Photodynamic therapy uses locally or systemically administered photosensitizers in which they are irradiated at the wavelength of that photosensitizer in order to generate reactive oxygen species and affect only the target tissue[22]. The advantage is that this photosensitizer does not accumulate in the core[22]. Photothermal therapy also uses photosensitizers that after being irradiated generate heat for the destruction of target cells[22]. Functionalization with other compounds like chlorine e6, carbon nitride, L-cysteine, m-phenylenediamine and copper can improve the ability to locate and destroy tumor cells, enhancing the efficacy of radiation[6]. Overall, CD show great potential in various applications and warrant further research in the field of cancer treatment[6].

For this study, we used D-fructose as the carbon source via microwave irradiation by bottom-up method. To the best of our knowledge, fructose was never previously described in the literature as carbon source for the formation of CD.

# Chapter 2 – Breast Cancer

Breast cancer (BC) is the most common and deadly cancer in the female population worldwide[3]. It is associated with the formation of tumors with heterogeneous characteristics. Breast cancer can be classified according to its location, histological grade, invasiveness and the presence of hormonal and HER2 receptors[34,35].

There are several risk factors able to promote tumorigenesis and BC development[35,36]. Modifiable and non-modifiable factors can include sex, age, reproductive life, obesity and family history namely mutations at the BRAC1 and BRAC2 genes[35,36].

Breast cancer can be classified according to the molecular subtype which presents the receptor status. There are 4 molecular subtypes: luminal A and B, HER2 and triple negative[37]. The most incident is luminal A with better prognosis and lower tumor reappearance rate[37].

Several factors can influence the most adequate treatment strategy for the patient in question, including age, menopausal status, molecular subtype consistency of the breast tissue, the development of the BC and metastatic rate[38].

Preliminary studies on CD observed a promising result in the treatment of breast cancer with less toxicity and side effects. The use of CD in diagnosis improves the quality of the techniques and in turn, more accurate results[12].

## 2.1 Epidemiology

BC is the most prevalent cancer with a high mortality and morbidity rate in the female population worldwide. In 2020, 684996, corresponding to 15.5% of the world's female population, were diagnosed with BC and 2261419, corresponding to 24.5% of the female population, portend BC mortality (**figure 3**)[3].

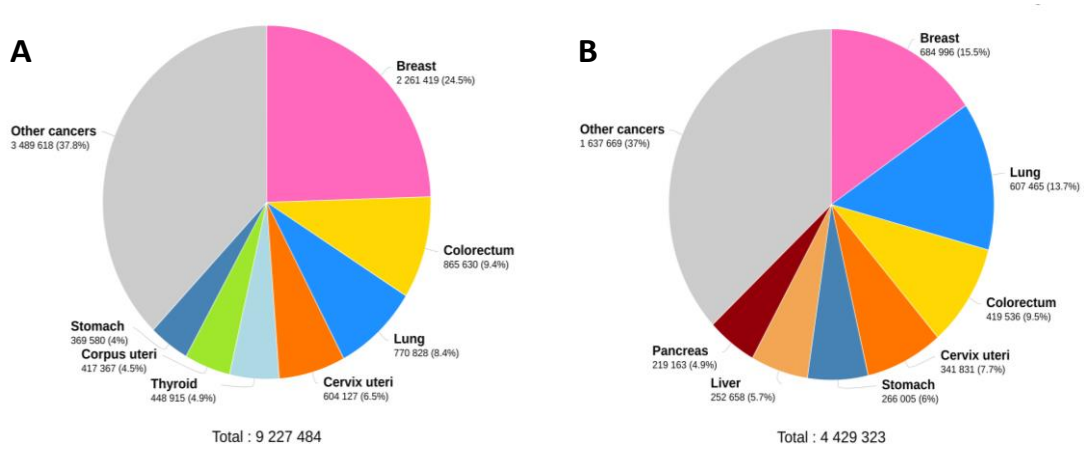


*Figure 3 - Estimated number of new cancer cases (A) and deaths (B) in 2020 in the world for the female population.*

## 2.2 Molecular Classification

In terms of classification, there are several representative types of BC based on molecular subtypes. According to the receptor status of hormonal and HER2 receptors, BC can be classified in luminal A, luminal B, HER2 (Human epidermal growth factor receptor 2) positive and triple

negative (**figure 4**)[37]. Molecular classification is based on the expression of both hormonal receptors: estrogen receptor (ER) and progesterone receptor (PR) and also according the HER2 positivity.

Molecular classification can include basal markers such as cytokeratin 5/6 (CK5/6) and human epidermal growth factor receptor (EGFR) present in the basal-like and claudin-low molecular subtypes and the Ki-67 proliferation index[37]. CK5/6 is a crucial molecular marker for EGFR identification[39] which plays a key role in tumor cell proliferation, since it is associated with cell movement, invasion and angiogenesis[39].

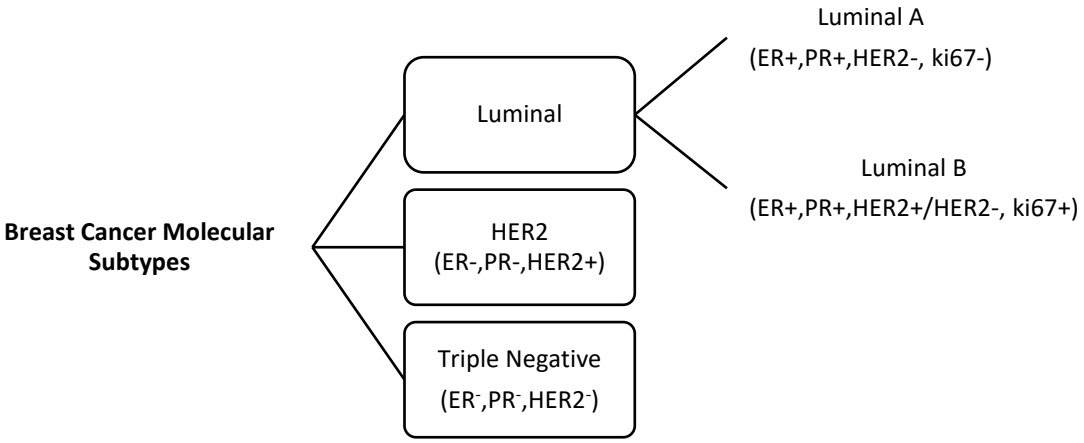


*Figure 4 - Schematic representation of the molecular subtypes of BC.*

Luminal subtype affects the inner luminal zone of the breast epithelial cells and it is distinguished into luminal A and luminal B[37,40]. Luminal A is the most common and is characterized by high expression of ER and PR and negative HER2 and Ki67[37]. Usually, the tumors have low histological grade, little mitotic activity, low ability to change the shape and size of the cell nucleus and normally differentiate into invasive ductal and lobular histological type[40,41]. Given the characteristic features of this molecular subtype, is usually associated with a good prognosis[40]. Luminal B is characterized by positive expression of ER, PR and ki67 and positive or negative expression of HER2[37]. Luminal B exhibit a more aggressive phenotype, high histological grade, high proliferative index and is associated with a poorer prognosis[40]. Compared to luminal A, it has a lower survival rate and is more likely to relapse[40].

The HER2-enriched molecular subtype is characterized by high HER2 expression. HER2 belongs to the four-membrane tyrosine kinase family and the receptor is encoded in the HER2/neu also known as ErbB2 gene. This tumor type has a high proliferative capacity as well as high histological and nuclear grade[40].

Triple negative accounts for 20% of BC cases and is quite heterogeneous due to its negative ER, PR and HER2 expression characteristics[41]. Biologically, is associated with a poorer prognosis due to its aggressive phenotype.[41].

## 2.3 Detection and prognosis biomarkers in BC

Biomarkers are crucial in the diagnosis and treatment of BC[42]. In addition, they are associated with tumor progression, disease risk, metastatic tumors, distinction of malignant and benign cancers, prognosis characterization, cancer status and response to treatment[42]. There are several types of biomarkers distributed according genomic, metabolomic, transcriptomic and proteomic profiles[43]. The best-known genetic variations are in the CYP1A1, RAD1, BRAC1 and BRAC2 genes[43]. BRAC1 and BRAC2 function as tumor suppressors, however, genetic alterations can lead to hereditary BC risk[43]. ATM, TP53, BRIP1, CHEK2, PTEN, MAP3K1, PALB 2, FGFR2 and TGFB1 are genes most used for BC onset[43]. Messenger RNA and micro-RNA have been described as potential biomarkers, extracted from blood samples taken by minimal invasive techniques such as liquid biopsy[43]. In terms of proteins, there are a variety of them that serve as biomarkers for BC diagnosis such as EGFR, HER, p53, CA125, CA19-9, CA15-3, CA242, CA27.29, CA15-9, EGF, VEGF and carcinoembryonic antigen (CEA)[43]. Metabolites are also evaluated in cancer, since they provide information about the progression, risk and detection of BC[43].

The most common biomarkers in BC are ER, PR, HER2[41]. However, there are other biomarkers such as ki67, claudins, E-Cadherin, cyclin D1 (CD1), circulating tumor cells (CTC), PD-l1, TILs, Mib1, p53 and tumor-associated macrophages[41,42].

The BRAC1 gene encodes a nuclear protein that has the function of maintaining genomic stability[35]. This gene has the ability to bind to others that allow communication with RNA polymerase II that binds to histone deacetylase and disrupts the process of transcription, repair, or DNA recombination[35]. BRAC1 and product of BRAC2 together can repair the DNA double-strand by homologous recombination[35]. Other genes such as TP53 and PTEN are associated with a BC risk of 54% and 25-50% respectively[35]. p53, a gene associated with the TP53 mutation, is a protein that has the function of cellular homeostasis, genome maintenance through cellular stress responses that can lead to cell cycle arrest, apoptosis, DNA repair and cellular senescence[41]. Suppression of this gene is found in early BC[41]. It was also found that mutations in ATM, BRIP1, CHEK2 and PALB2 genes exhibit a moderate risk for BC development[35].

ER belongs to the nuclear steroid receptor group and functions as a transcriptional regulator. When ER is activated by the hormone it forms dimers which in turn gives rise to two isoforms of ER, ER-α homodimer presents on human chromosome 6 and ER-β heterodimer present on human chromosome. This receptor plays a role in cell growth, proliferation and differentiation. The expression of ER defines the treatment strategy. Global guidelines advice that $ER^+$ BC patients should be submitted to endocrine therapy. Higher levels of ER are associated with better prognosis due to efficacy in the response to endocrine therapy[44].

PR is a member of the ligand-activated nuclear receptor family and is encoded by the PGR gene. It can be expressed in 3 isoforms PR-A, -B and -C with distinct functions[44]. While the action of -A and -B are affected by the behavior of the signal transduction pathway initiated by peptide growth factor, -C is associated with inhibition of -B in utero via the receptor tissue[44]. PR, when in the presence of progesterone, interacts and stimulates alteration of the binding site between ER and chromatin which causes alteration of genes that become able to model cell cycle arrest, apoptosis and differentiation[44]. Low PR expression indicates poor prognosis and tumor relapse; high PR levels are associated with lower overall survival (time between diagnosis and death of cancer patient), lower time to relapse and a more aggressive treatment[41,44].

HER2 is a crucial marker in BC and belongs to the epidermal growth factor receptor family[44]. Normally, this family alters the gene transcription of membrane proteins and intracellular signaling mediators by phosphorylation through cell-to-cell contact via transduction signals on external growth factors[44]. It is usually expressed in epithelial cells of distinct organs such as lung, pancreas, breast, prostate and bladder and overexpressed in tumor cells[44]. This biomarker is prognostic for the time to reappearance and overall survival of patient with BC[44].

Ki-67, related to cell division and growth and ribosomal RNA synthesis, is a non-histone nuclear cortical protein[44]. Its expression varies depending on the phase of the cell cycle, peaking most often in mitosis[44]. Its expression is positively associated with cell proliferation in which the higher its expression, the greater the cell division[37]. It is a prognostic tool used in BC relapse and response to chemotherapy[44]. High levels of ki-67 are associated with larger tumors more advanced histological grade, lymphocytes infiltration, lower overall and disease-free survival[44].

It was recently described the importance of claudins in BC progression, given their role in the cell signaling pathway of the epithelium-mesenchymal transition (EMT) and ER signaling modulation. Claudins are proteins that form tight junctions, are involved in cell-to-cell adhesion and communicate with other proteins to form structures with permeability and ionic selection capabilities. The expression of this marker is defined by the presence of growth factors such as TGF-B and the cytokines that are present in the EMT[45].

E-cadherin is a transmembrane glycoprotein expressed on epithelial cells, has homophilic adhesion capacity and is considered a tumor suppressor protein[46]. E-cadherin is a transmembrane protein that when downregulated leads to metastasis[47].

There are also serum tumor markers, essentially, CEA, CA-15-3 and CA125 associated with clinicopathological features of BC aggressive behavior. CEA and Ca-15-3 are glycoproteins and CA125 is a result of the MUC1 gene that plays an important role in multicellular survival pathways associated with the ovary and breast. CEA is associated with cell adhesion and indicates inflammation or cancer. CA-15-3 is a tumor biomarker associated with glycosylation. High levels of CEA and CA-15-3 is correlated with the tumor burden and metastasis. CA-125 is also biomarker of other type of cancer, specifically, colorectal[44].

CTC are rare tumor cells, present in the peripheral blood and associated with tumor development[44]. High levels have lower survivability and resistance to treatment is due to poor treatment response[44].

CD1 is one of the molecules that regulate the cell cycle and the activity of the kinase-dependent cyclins that promote cell cycle function from G1 to S. When this molecule binds to CDK4 and CDK6 there is hyperphosphorylation of the retinoblastoma protein that loses the ability to communicate with the transcription factor E2F leading to its activation which promotes cell proliferation. High expression of cyclin D is associated with poor prognosis, violent behavior and increased migration capacity[44].

## 2.4 Risk Factors

BC risk factors can be divided into modifiable or non-modifiable factors. Non-modifiable factors include gender, age, family history, non-tumor breast disease, ethnicity, genetic mutations, pregnancy, breastfeeding, menstrual period, menopause, breast tissue density,

previous history of BC and previous radiotherapy. While modifiable factors are diethylstilbestrol, hormone replacement therapy, obesity, alcohol, smoking, vitamin insufficiency, exposure to artificial light and chemicals, diet and medications[36].

99% of cases of BC are diagnosed in women over the age of 50[35,36]. A family history of cancer poses a risk for people undergoing radiation treatment just as the onset of benign breast disease poses a higher risk of developing BC[35,36,48]. Caucasian women are most affected by this type of cancer[48]. As previously mentioned, family history is associated with the mutations of certain genes like BRAC1 and BRAC2 leading to an increased risk of BC[35,36]. Pregnancy is a process of great hormonal requirements where there is an increase in progesterone and decrease in estrogen, insulin, cortisol, insulin-like growth factor-1 androgen, human chorionic gonadotropin, corticotropin-releasing factor and IGF-1 binding protein[35,36]. Later pregnancies are a risk factor[35,36]. Early menarche is associated with lymph node appearance and worse prognosis[35,36]. Contrarily, early menopause decreases the risk of BC[35,36]. Regarding breast tissue density, the higher it is, the greater the risk of BC formation[36,48]. Radiation therapy is a treatment that can lead to the appearance of malignant tumors due to radiation exposure. In this case, the most common are patients under the age of 30[35,36].

Exposure to diethylstilbestrol, a medication to prevent miscarriage, increases the risk of BC as well as for the female descendent[36,48]. Hormone replacement therapy, antidepressants and antibiotics is also a risk factor[36]. Obesity is included in a high-risk factor for BC with larger tumors and with lymph node metastases[36]. Obesity is responsible for a low chronic state of inflammation, alterations in circulating hormones due to the expression of aromatase which can stimulate pro-carcinogenic events[36]. The consumption of processed foods has a high risk for the development of BC, since they are composed of large amounts of sodium, fat and sugar with the risk of developing obesity associated with the risk of BC[36]. Alcoholic beverages consumption induces metabolic dysregulation, increased estrogen levels associated with the risk of carcinogenesis[36]. Due to the composition of the carcinogens found in tobacco, mutations in the p53 gene can occur, representing a risk for the development of breast cancer[36]. Studies have shown that low vitamin D may be a risk factor for developing BC[36]. Exposure to chemical substances or substantial physical alterations represents a risk factor for BC. In the presence of BC, it affects the tumor microenvironment leading to epigenetic modifications which in turn lead to pro-carcinogenic events causing breast carcinogenesis such as exposure to artificial light, processed foods, some types of drugs such as antidepressants, etc[36]. Drugs can also pose a risk of BC such as taking antibiotics, antidepressants, statins and also non-steroidal anti-inflammatory drugs like aspirin, ibuprofen[36]. Another factor related to the risk of BC is the exposure to artificial light that can be justified by the stoppage in the melatonin rhythm that can lead to epigenetic modifications[36].

## 2.5 Detection

BC detection is performed with different methods such as mammography, magnetic resonance imaging (MRI) without and with dynamic contrast, elastography, diffusion weighted and MRI spectroscopy, positron emission tomography (PET) and in conjunction with computed tomography (CT), biopsy, gamma imaging and ultrasound[38].

Mammography is an x-ray method used for diagnosis and screening. This technique allows the identification and evaluation of breast neoplasia. Preliminary studies with the use of gold

nanoparticles have improved the contrast of this exam[38]. In addition, mammography is also used as an early diagnosis of BC. It is the most used technique in screenings carried out. In Portugal, screening is carried out by the Liga Portuguesa contra o Cancro women aged between 50 and 69.

MRI allows the obtaining images of the structures inside the breast, the size of the tumor and metastasis status. MRI uses contrast agents to specifically visualize tumor cells. The contrast agents usually used are $Fe_3O_4$, gadolinium (III) and Mn (II). They can also be encapsulated with polymeric carriers targeting in order to decrease toxicity outside the target zone. Dynamic contrast-enhanced MRI works with an intravenously injected paramagnetic contrast agent that allows tissue enhancement. It allows imaging of the vessels, interstitium and lesion compartments. Using this technique in conjunction with informatic processing molecular subtypes of BC can be identified. MRI elastography is a technique that provides tissue mechanical properties *in vivo*. Under induced stress, this technique allows the viscoelastic properties of breast tissue to be determined. However, it is known that in BC, the tissues are stiffer due to the increased number of cells and the deposition of collagen and proteoglycans[38].

Diffusion-weighted imaging refers to the contrast enhancement of the MRI technique from the diffusion of water molecules. This technique, besides presenting no risk of radiation exposure, is also ideal for evaluating the differentiation of benign and malignant lesions and selecting the most suitable treatment strategy. It also enables the recognition of cancers in breasts with high mammary density. However, this technique is not widely used in the clinic due to image quality problems and variable sensitivity compared to MRI[38].

Magnetic resonance spectroscopy provides information on the chemical spectrum of the area under study by using a high-intensity magnetic field that focuses on body fluids, cell extracts and tissue samples[38].

PET has been widely used in the field of oncology. PET utilizes radiotracers to evaluate metabolism in vivo with resource to a precise glucose analog, 2-deoxy-2-(18F)fluoro-D-glucose (FDG). This technique is based on the tumor metabolism and its increased glucose uptake. This radiotracer penetrates the cells via glucose transporters and is taken up to a greater extent by tumor cells. The higher the radiotracer uptake, the worse the prognosis. The combination of PET and CT results in a detailed imaging, mainly to diagnose and evaluate the development of cancer, the best treatment and its effectiveness[38].

Breast-specific gamma imaging evaluates metastatic tumors located in the axillary lymph nodes. Usually works with a radiopharmaceutical injected into the bloodstream and a camera for visualization. The radiation exposure is the uttermost disadvantage associated[38].

Ultrasound is a complementary technique without radioactive exposure that evaluates breast tissue density and non-visible areas of the breast. This technique is usually combined with other techniques (like ultrasound-guided biopsy and ultrasound elastography) to improve efficacy. Ultrasound elastography allows assessing tissue thickness in order to differentiate benign and malignant lesions[38].

Biopsy is an invasive diagnostic technique. It allows the removal of liquid samples from different areas of a nodule or solid samples (tissue samples). The liquid samples will be analyzed

according to the components found in the tumor cells and the nodule will be classified as benign or malignant. In addition, they can be collected multiple times and allow sampling of localized and metastatic tumors. Whereas tissue samples are collected only once at diagnosis or during tumor resection and molecular information about the tumor is limited[49,50].

In BC diagnosis, CD have been investigated as contrast agents to improve image quality of conventional techniques. In MRI, superparamagnetic iron oxide nanoparticles were used in preliminary studies as a contrast agent. These nanoparticles can lead to inhibition of new blood vessel formation (angiogenesis) and instigate autophagy of endothelial progenitor cells. In large doses, it can cause damage at the cytoskeleton level and decrease cell proliferation. However, they can damage cells at the DNA level, damage proteins and promote inflammation. An alternative are gold nanoparticles, which are less toxic. The most commonly used agent is gadolinium, however, it has a limited life span in the body, as does manganese. Manganese oxide nanoparticles showed promising results. Ultrasound has poor sensitivity and specificity, to improve this downfall, targeted microbubbles are being the subject of recent research. Usually in this type of technique, contrast agents such as echogenic liposomes, perfluorocarbon nanodrops and solid nanoparticles (not microbubbles) and gas filled microbubbles are used. Computed tomography disadvantage is associated with low resolution with problems differentiating soft tissue with the same density. To improve contrast, are used gold nanoparticles because of their high X-ray absorption capacity allow better visualization of the tissue[51].

Nanoparticles in optical imaging allow for more visible fluorescence, greater stability, lifetime in the body and accumulation in the tumor[51].

## 2.6 Treatment

BC treatment always depends on the patient's health and age as well as patient's choice, doctor's indication and stage of the tumor. In the presence of localized tumor, the main goals are the elimination of tumor cells, prevent metastasis and its reappearance. In an advanced stage, which include large tumors and the presence of metastasis is usually recommended a neoadjuvant therapy. There are systemic treatments where chemotherapy, endocrine therapy, HER2 targeting and immunotherapy are incorporated and there are also local treatments where surgery and radiotherapy are applied. Nanoparticle treatments have recently been developed to combat the contradictions of conventional treatments[12].

Chemotherapy is a cytotoxic therapy that affects tumor cells at different stages of the cell cycle[12]. It can be adjuvant chemotherapy in which the patient undergoes surgery and then chemotherapy if they have lymphatic metastases or a high probability of BC reappearance and neoadjuvant when applied before surgery. Neoadjuvant treatment commonly decreases the size of the tumor and increases the ability to conserve the breast. Usually, drugs such as doxorubicin, epirubicin, PTX, docetaxel, cisplatin, carboplatin and cyclophosphamides are used that can be given orally, intravenously injected, or intrathecally. The use of several drugs can enhance the antitumor effect[12].

Endocrine therapy is used in positive hormone receptors BC. It allows to hinder estrogen function or decrease levels to prevent stimulation of BC cells. Drugs such as tamoxifen and

toremifene (selective ER modulators), fulvestrant (selective ER degrader) and aromatase inhibitors such as letrozole, anastrozole and exemestane are used[12].

Immunotherapy consists of stimulating the patient's defense system to promote an immune response and eliminate malignant cells. This type of therapy is also promising for the prevention of metastases and reduction of BC recorrence[12].

Surgery may involve breast-conserving procedures or total removal of the breast (mastectomy)[52]. Breast-conserving surgery includes procedures such as lumpectomy, quadrantectomy and partial mastectomy[53]. Lumpectomy is a procedure that removes only the localized tumor and is not as invasive as mastectomy[52]. It is the ideal treatment when there is a small and localized tumor without metastases, inflammation and exposure to radiotherapy[53]. A larger part of the breast can also be removed, a quadrant (quadrantectomy) in which there is removal of the breast tissue near the pectoralis muscle[53]. One of the prognostic markers is the status of the axillary lymph node[12]. Partial mastectomy is considered a breast-conserving procedure, since only the tumor, some surrounding breast tissue and the lining of the breast muscle and some lymph nodes, both located underneath the tumor, are removed[54].

Mastectomy is divided into total, modified radical and radical. Total mastectomy involves the complete removal of the breast tissue. Modified radical mastectomy includes the complete removal of the breast as well as the removal of axillary lymph nodes. And finally, radical mastectomy refers to the removal of the breast, breast muscles and fascia and all axillary lymph nodes[54].

The sentinel lymph node technique has been widely used since it avoids the removal of many nodes and consequently fewer side effects[12]. Is performed to determine the metastatic state of the BC. In conjunction with conventional axillary lymph node dissection, improves post-operation complications. In other words, it has a fundamental role in the diagnosis of BC and in the effective treatment. It allows over treatment like unnecessary surgeries[38].

Although there are several conventional treatments, there are associated contraindications, mainly, their aggressive side effects, drug resistance, high toxicity and likelihood of developing other diseases. To improve the aggressive side effects of anti-tumoral treatments nanomedicine has been investigating nanoparticles with promising antitumor capabilities and with less risk of contradictions. Combining chemotherapy with photodynamic and photothermal therapy has shown promising better results. Chemodynamic therapy is a method that produces highly toxic hydroxyl radicals that cause oxidative stress damage and cell death. This type of therapy is specific and selective towards the target (tumor) cells, has low cytotoxicity and fewer side effects. This technique in conjunction with chemotherapy increases the action of chemotherapy drugs and decreased their side effects[12].

Oxidative stress is often a target for BC treatment, since it is known that there is greater tumor survival under conditions of oxidative stress.

# Chapter 3 – Oxidative Stress

Tumor cells are characterized by elevated reactive oxygen species (ROS) and downregulation of the cellular antioxidant enzyme system, which results in malignant transformation[55]. Genetic mutations can stimulate the production of high levels of ROS. In normal cells these conditions cause oxidative stress, but in tumor cells occurs an increased growth due to DNA alterations, genomic instability and reprogramming of tumor cell metabolism[56].

The influence of low and moderate levels of ROS in the tumor microenvironment leads to angiogenesis which promotes tumor proliferation and survival[55]. In addition, high levels of ROS can act as anti-tumor molecules as they promote cell death pathways such as apoptosis, necroptosis and ferroptosis[57].

## 3.1 ROS

ROS are highly oxidative, partially reduced, oxygen-derived reactive molecules produced by molecular processes and contribute to intracellular oxidative stress[58,59]. ROS can be considered free radical species such as the superoxide ($O^{\bullet -}_2$), oxygen radical ($O^{\bullet\bullet}_2$), hydroxyl ($OH^{\bullet}$), alkoxy radical ($RO^{\bullet}$), peroxyl radical ($ROO^{\bullet}$) or non-radical like hydrogen peroxide ($H_2O_2$), hypochlorous acid (HOCl), hypobromous acid (HOBr), ozone ($O_3$), singlet oxygen ($^1O_2$), organic peroxides (ROOH), aldehydes (HCOR)[60,61].

Mitochondria are a significant source of ROS in cells, contributing to oxidative stress. Electron transport chain (ETC) on the inner mitochondrial membrane generates most mitochondrial ROS during oxidative phosphorylation[62].

The reduction of oxygen to $O^{\bullet -}_2$ occurs due to the loss of electrons from complex I and III of ETC which causes dismutation to $O^{\bullet -}_2$. ECT activity is also regulated by a transcription factor STAT3 in response to the cytokine's interleukins IL-6 and IL-10. NO and $Ca^{2+}$ are endogenous regulators of ROS production in mitochondria. ROS levels decrease when $Ca^{2+}$ levels increase. What induces a $Ca^{2+}$-dependent increase in mitochondrial levels is TNF-α which causes the release of the receptor 1 of this transcription factor[62].

Factors such as HIF-α play an important role in oxidative stress. In the reduction of ROS levels, HIF-α is present which stimulates pyruvate dehydrogenase kinase 1 which leads to the detour of pyruvate from mitochondria, can lead to mitochondrial autophagy and also induce the expression of microRNA-210 which blocks oxidative phosphorylation. HIF-α is also regulated by low levels of mitochondrial ROS adapting more easily to the hypoxic state. Pro-inflammatory cytokines are regulated by moderate levels of mitochondrial ROS leading to activation of inflammasome and mitogen-activated protein kinase. High levels of mitochondrial ROS led to apoptosis and autophagy by oxidation of mitochondrial pores and oxidation of autophagy-specific gene 4 (ATG4), respectively[62].

Mitochondria plays a relevant role in the loss of caveolin 1 (cav-1) in tumor-associated fibroblasts, which is related to early tumor recurrence, metastasis, tamoxifen-resistance and increased tumor growth. ROS production in mitochondria plays a central role in cell proliferation and quiescence. Mitochondrial ROS exchange by the antioxidant enzyme MnSOD (manganese superoxide dismutase) controls pro- and anti-tumorigenic signaling. A decrease in the activity of this enzyme leads to an increase in $O^{\bullet -}_2$ production. In a high proliferative state, cells can switch

to quiescence mode when MnSOD activity increases leading to an increase in $H_2O_2$. Increased oxidative stress in tumor cells is also related to inhibition of the antioxidant response of thioredoxin reductase in mitochondria that reduces to oxidized thioredoxin and reacts with ROS[62].

The increase in lactate may occur due to the conversion of glucose to lactate by the activation of hexokinase 2 and pyruvate dehydrogenase kinase 1 that occurs due to HIF-α and MYC. The Warburg effect is an acknowledged mechanism that tumor cell acquires for survival advantage over normal cells. It consists in an aerobic glycolysis in the presence of oxygen and functional mitochondria[63].

Warburg effect increases ROS levels as lactate, which is produced in excess and has no antioxidant properties, is released into the tumor microenvironment via monocarboxylate transporters. Hexokinase II and NADPH play a key role in preventing tumor cells from reaching cytotoxic levels by increasing oxidative stress[62]. HIF-1α, beyond its role in hypoxia and angiogenesis is also a regulator of the Warburg effect. It is coactivated by PKM2 induced by prolyl hydroxylases. Regulate the MYC proto-oncogene that produces the MYC protein and has the function of regulating genes that are present in energy production and cell growth and proliferation. Increased glucose influx and glycolytic rates result from HIF-1alpha and MYC independently activating glucose transporter 1 and lactate dehydrogenase A (LDH A). LDH is an intracellular enzyme that plays a key role in the reversible conversion of pyruvate to lactate as well as NADH to NAD+. It is the main oxidoreductase enzyme in glycolysis that stimulates the transfer of electrons from a donor molecule to a receptor[62].

NOX, a subunit of NADPH oxidases, performs electron transfer from NADPH to $O_2$ resulting in ROS. The influence of NOX-derived ROS promotes cell survival and genomic instability. Each isoform of NADPH oxidases has a different origin and impact in ROS formation. Biological membranes transfer electrons to NOX which produce $O^{\bullet-}_2$ that is converted to $H_2O_2$. MAPK signaling, phagocytosis, apoptosis, neutrophils, senescence and cell growth are activated by $H_2O_2$. ECT is an oxidase that produces $O^{\bullet-}_2$. $H_2O_2$ also plays a role in oxygen sensing which, in a hypoxic state, stimulates HIF-1α and angiogenesis. In addition, the generation of eNOS (endothelial nitric oxide synthase) is realized from the conversion of xanthine dehydrogenase to xanthine oxidase[62].

In the endoplasmic reticulum, ROS are produced by the catalytic processes of oxidoreductase ERO1 and NOX. Oxidative protein folding is the primary source of ROS as its transporter piece ERO1 uses molecular oxygen to initiate the redox state and can lead to the formation of disulfide bridges in proteins. Peroxiredoxin 4 and the glutathione peroxidases GPx7 and GPx8 reduce H2O2 from ERO1 and NOX and prevent its release from the endoplasmic reticulum. The constant stress of the endoplasmic reticulum by unfolded proteins (UPR) can be reduced by the influx of GSH. URF is activated by the production of ROS which inactivates the conversion of -SH group of cysteine to a persulfide group or to -SSH of protein tyrosine phosphatase 1B. This leads to phosphorylation and activation of the PKR-derived endoplasmic reticulum kinase (PERK) which is important in cellular homeostasis by regulating autophagy and apoptosis mechanisms[62].

## 3.2 Antioxidant Mechanisms

Antioxidants play a key role in minimizing the damage caused by oxidative stress. Free radicals act as a threat to cellular elements affecting the cell membrane but also DNA and proteins. ROS can be formed from by-products of normal cellular metabolism and play a key role in cellular homeostasis and signaling. They can also be products of plasma membrane specific oxidase via growth factors and cytokines, are involved in the regulation of gene expression and in signaling pathways function as secondary messengers. Antioxidants can neutralize the previously described damage[62].

To maintain ROS control, cells have potent antioxidant mechanisms namely antioxidant enzymes that regulate ROS levels to physiologically accepted levels. Antioxidant enzymes play a key role in transforming free radicals into more stable and harmless molecules. They can be endogenous enzymatic or non-enzymatic antioxidants and exogenous antioxidants. Superoxide dismutase (SOD), catalase, glutathione peroxidase and reductase and heme oxygenase belong to the endogenous antioxidant enzymes. Glutathione, thioredoxin and melatonin are considered endogenous non-enzymatic antioxidants. Vitamins A, C and E, minerals and polyphenols are exogenous antioxidants[60].

SOD is a metalloenzyme that converts $O^{\bullet -}_2$ into $H_2O_2$ and $O_2$. It uses cofactors such as copper, zinc, manganese or iron. There are different SOD isoforms located in different organelles with different biological regulations. In the mitochondrial matrix manganese-SOD converts $O^{\bullet -}_2$ into $H_2O_2$ as well as copper/zinc-SOD in the cytosol[64].

Catalase converts $H_2O_2$ into $H_2O$ and $O_2$, inoffensive molecules to cells, is present in the cytosol and peroxisome[64].

Glutathione is an important antioxidant system as it defends cells from oxidative stress. This happens due to the elimination of disulfide bridges located between cytoplasmic proteins and cysteines. During this process, glutathione is oxidized to glutathione disulfide. Glutathione peroxidase degrades $H_2O_2$ and organic hydroperoxides while reductase leads to the reduction of glutathione disulfide which replenishes glutathione levels[64].

In short, oxidative stress is related to tumor progression. Higher levels of ROS are associated with greater tumor survival. It is known that CD most affect the toxicity, proliferation, migration and injury of tumor cells. To this end, we evaluated some of the most important enzymes (SOD, catalase and total glutathione) to see if this influence is associated with oxidative stress pathways.

# Chapter 4 – Aims

The aim of this study is to synthesize and characterize fructose-derived CD according to size, morphology, structure, functional groups and fluorescence.

Evaluate the influence of CD on breast epithelial and breast tumor cell lines regarding impact on viability, proliferation, migration and injury to evaluate their antitumor effect as potential onco-therapeutics for BC.

Analyze the key antioxidant enzymes, namely SOD, catalase and total glutathione (GSH) and the intracellular enzyme lactate dehydrogenase and the antioxidant activity from 2,2-Diphenyl-1-picrylhydrazyl (DPPH).

# Chapter 5 – Materials and Methods

## 5.1 CD

### 5.1.1 Synthesis

A previously described protocol[65] with minor alterations was used to CD synthesis. In summary, 11 g of D-fructose (Panreac, E.U.) was added to 16 mL of deionized water. After homogenization, 55 mL of polyethylene glycol 200 (DEG) (Scharlau) was added. From the final solution, 13 mL was allowed to react in a conventional microwave (Becken, 700 W, Med High temperature) for 5 min.

### 5.1.2 Purification

#### 5.1.2.1.Dialysis

Dialysis was performed using a dialysis membrane (Spectra/Per Dialysis membrane Biotech Ce Tubing MWCO: 100-500 Da) against deionized water for 24h. The main objective of this procedure is to eliminate the organic solvent (DEG).

#### 5.1.2.2.Centrifugation/Filtration

50 mL of dialyzed CD were centrifuge at 21000 g for 2h. Afterwards, the supernatant was harnessed and filtered through a filter membrane of 0,22 µm to remove larger particles. The obtained solution was filtered on a 3 kDa MWCO centrifugal filter (Vivaspin) to obtain homogeneous particles smaller than 3 kDa.

#### 5.1.2.3.Lyophilization

The sample was frozen at -80 °C for 24h. It was then placed in the freeze-dryer for 3 days at -86 °C and 200 mTorr. A caramel-like compound was obtained, easily handled in characterization techniques and cellular assays. All purification processes are described in **figure 5**.

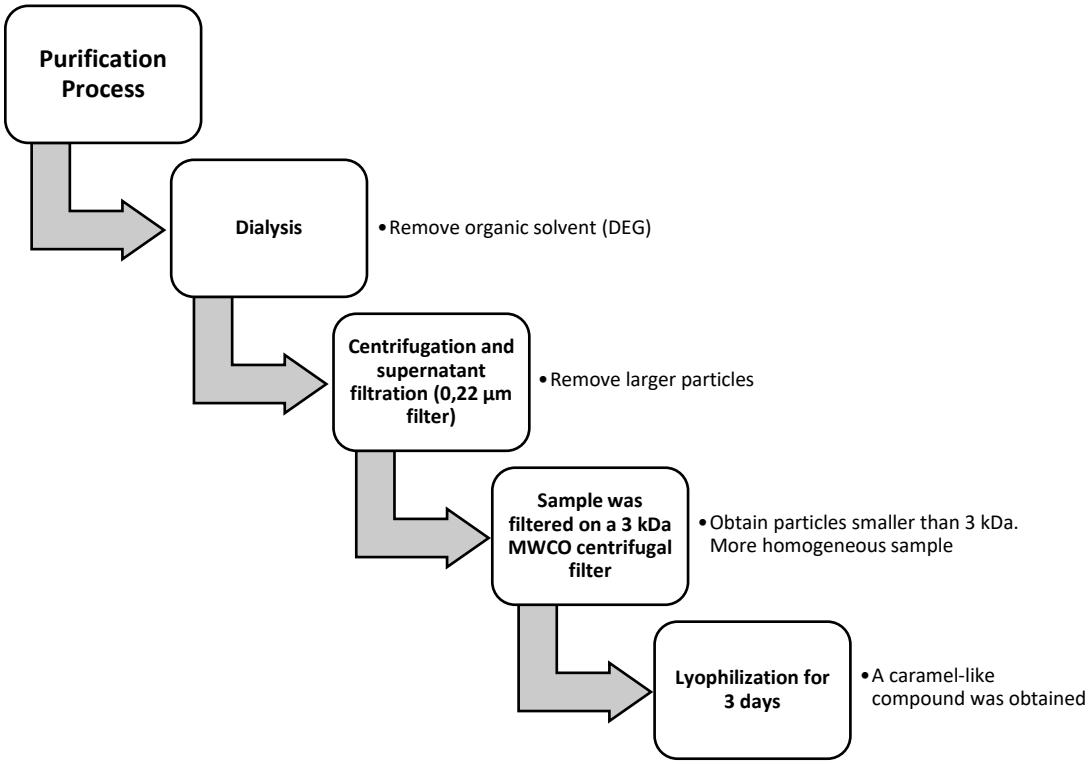


*Figure 5 - Schematic diagram representing the purification processes of CD.*

## 5.1.3 Characterization

### 5.1.3.1.Homemade fluorometer

The fluorometer was equipped with a detector USB 2000 Ocean Optics, an optic fiber connected to a cube tip (Cuv Sample Holder of 4 pathways) QP600-2-VIS-BX-Ocean Optics and an excitation led of 405 nm. This allowed the measurement of the fluorescence samples.

### 5.1.3.2.Spectrophotometer

The absorbance measurement of the samples was performed using a cuvette with 2.4 mL of sample in the spectrophotometer (Nanocolor-Advance Macherey-Nagel). The absorbance was measured at a wavelength between 360 nm and 800 nm.

### 5.1.3.3.Dynamic light scattering (DLS)

Hydrodynamic diameter (DH) and zeta potential were performed using a Malvern Zetasizer Nano ZS (Malvern, UK). 3 measurements for each sample were taken, at 25 °C, with light detection at 273° (DLS) and electrophoretic light scattering at 17°.

### 5.1.3.4.Transmission Electron Microscopy (TEM)

This technique was performed at @INL, Braga according to internal protocols. Morphology, size and structure of the CD was determined with this technique. The equipment used was Jeol JEM-2100-HT, 200 kV analytical electron microscope.

### 5.1.3.5.Fourier-transform infrared spectroscopy (FTIR)

FTIR allowed the detection of functional groups on the surface of CD. Since the freeze-dried sample is a caramel-like compound, to obtain the infrared spectrum it was necessary to perform a parallel technique using two circular NaCl windows. The spectrum was obtained from a Nicolet 6700 FT-IR Spectrometer (Thermo Electron Corporation, USA).

## 5.2 Cell culture

### 5.2.1 MCF-10A and BT474 cell lines

#### 5.2.1.1.Cell culture

Human mammary epithelial cells MCF-10A (American Type Culture Collection, Manassas, VA) were cultured in Dulbecco's Modified Eagle Medium (DMEM)/Ham's F-12 (GIBCO-Invitrogen, Carlsbad, CA) supplemented with 100 ng/ml cholera toxin, 20 ng/ml epidermal growth factor (EGF), 0,01 mg/ml insulin, 500 ng/ml hydrocortisone and 10% horse serum. All of the growth factors were purchased from Sigma (St. Louis, MO, USA)[66]. The cells were used between passages 25 to 36. Human breast carcinoma cells BT474 were cultured in DMEM (Sigma–Aldrich, St. Louis, USA), supplemented with 20% Fetal Bovine Serum (FBS, Invitrogen Life technologies, Waltham, USA), 1% penicillin/streptomycin (Invitrogen Life technologies, Waltham, USA) and 3,7 g/L sodium bicarbonate and maintained at 37 °C in a humidified atmosphere containing 5% $CO_2$. The cells were used between passages 13 to 38. Treatments were performed using respective medium, without supplementation, using different concentrations of CD.

#### 5.2.1.2.Metabolic Activity Assay (MTT)

BT474 and MCF-10A ($1 \times 10^5$ cells/mL) were cultured with CD at a stock solution of 50 mg/mL for 24h and the IC50 was analyzed using a range of concentrations from 1 to 10 mg/mL. Cells were subjected to MTT [3-(4,5-dimethylthiazol-2-yl)-2,5-diphenyl tetrazolium bromide] assay, an index of cell viability and cell growth. Cells were incubated with MTT solution (Abcam, Cambridge, UK) at a final concentration of 0,5 mg/mL for 3h and then lysed in DMSO. Optical density was measured at 550/560 nm in a UV–VIS spectrophotometer (MultiSkan Ascent, Thermo Fisher, Massachusetts, USA). The background absorbance was subtracted. All samples were assayed in triplicates of three replicates. The mean value for each experiment was calculated. The results are given as mean ± standard deviation and are expressed as percentage of control which was considered to be 100%.

#### 5.2.1.3.BrdU Proliferation Assay

This method is based on the cell ability to incorporate 5-bromo-2'-deoxyuridine (BrdU) into cellular DNA during cell proliferation. Then, incorporated BrdU is detected using an anti-BrdU antibody. BT474 and MCF-10A ($1 \times 10^5$ cells/mL) were cultured with CD concentrations close to the IC50 (5, 5.5 and 6 mg/mL) for 24h. Bromodeoxyuridine (BrdU) was incubated for 24h. The detection was performed using the colorimetric Cell Proliferation ELISA, BrdU (ab126556, Abcam, Cambridge, U.K.), according to the manufacturer's instructions. Control was standardized in all assays. All samples were assayed in triplicates of three replicates.

#### 5.2.1.4.Injury Assay

The injury assay (or scratch-wound assay) is commonly used to measure fundamental cell migration. Confluent MCF-10A monolayers on 24-plate well, were wounded with a 200-µl pipette tip and photographed. 24h after treatment, the migrated distance was photographed again under an inverted microscope (Nikon Instruments Inc., Melville, USA) at a 100× magnification. Scratch closure was determined by measuring the injury width with Image J

software (U. S. National Institutes of Health, Bethesda, USA). All samples were assayed in triplicates of three replicates.

The injury assay to BT474 was performed from culture-insert 2 well (250210, ibidi, Germany). In a 24-well plate, culture-insert 2 well was added and BT474 cells were cultured ($1x10^5$ cells/mL). After confluent BT474 on 24-plate well, culture-insert 2 well was removed with sterile forceps and photographed. 24h after treatment, the migration distance was again photographed on an inverted microscope (Nikon Instruments Inc., Melville, USA) at 100× magnification. Risk closure was determined by measuring the lesion width with Image J software (U. S. National Institutes of Health, Bethesda, USA). Control was standardized in all assays. All samples were assayed in triplicates of three replicates.

#### 5.2.1.5.Migration Assay

To assess migration rate on MCF-10A and BT474 cell lines, transparent PET membrane 8 µm pore size inserts (353097, Falcon, USA) were used in a 24-well plate in which treatment with serum-containing medium was added to the well and $5x10^4$ cells/well with serum-free medium was added to the insert. After 24h, cells were fixed with methanol for 30 min at -20 °C, stained with crystal violet for 20 min and pictures were taken from an inverted microscope (Nikon Instruments Inc., Melville, USA). The cells were counted and the percentage of migrated cells on the insert membrane was calculated. Control was standardized in all assays. All samples were assayed in triplicates of three replicates.

#### 5.2.1.6.Protein Extraction

Confluent MCF-10A and BT474 were exposed to described conditions for 24h. Cells were homogenized and lysed in NZYol. Proteins were extracted using the NZYol protocol, according to the manufacturer's instructions (NZYTech, Portugal). All samples were assayed in triplicate and stored at -80 °C for future assays. Quantification of total proteins was performed through the BCA kit-Pierce BCA Protein Assay Kit (#23225, Thermo Scientific, USA) according to the manufacturer's instructions. All samples were assayed in triplicates of three replicates.

## 5.3 Oxidative Stress

### 5.3.1 Antioxidant Enzymes

#### 5.3.1.1.SOD

SOD activity was measured using the protein lysate with a SOD determination kit (#19160, Sigma–Aldrich, USA) according to the manufacturer's instructions. Results were obtained according to the kit instructions, in percentage of inhibition of SOD activity. All samples were assayed in triplicates of three replicates.

#### 5.3.1.2.Catalase

Catalase Activity was measured using the protein extraction in a colorimetric kit (#ab83464, Abcam, UK) according to the manufacturer's instructions. Results were obtained in mU/mL of catalase activity. Calculations were performed according to the kit instructions. All samples were assayed in triplicates of three replicates.

#### 5.3.1.3.Total Glutathione (GSH)

Total Glutathione (GSH) was calculated using a Glutathione colorimetric detection kit (#EIAGSHC, Invitrogen, USA) using protein extract according to the manufacturer's

instructions. Results were expressed in µM. All samples were assayed in triplicates of three replicates.

### 5.3.2 Antioxidant Activity

#### 5.3.2.1.DPPH

The antioxidant activity was measured from DPPH (D4313, TCI, Japan) which is a free radical. The absorbance was measured at 515 nm in a UV-VIS spectrophotometer (MultiSkan Ascent, Thermo Fisher, Massachusetts, USA). DPPH radical scavenging capacity was expressed by Trolox equivalent (mM) [53188-07-1, Slovakia]. Trolox is a soluble analog of vitamin E and is an antioxidant. Therefore, it serves as a reference for the antioxidant capacity of the solution under study. All samples were assayed in triplicates of three replicates.

## 5.4 Cytotoxicity Assay

### 5.4.1 Intracellular Enzyme

#### 5.4.1.1.LDH

Cytotoxicity was measured by the release of LDH into the external environment stimulated by cell necrosis. Total LDH release was measured from the protein extraction by using Liquick color-LDH (#1-239, Cormay, Poland) according to the manufacturer's instructions. Calculations were performed following the kit instructions. All samples were assayed in triplicates of three replicates.

## 5.5 Statistical Analysis

The cellular, oxidative stress and cytotoxicity assays were performed in triplicate and the results were analyzed by one-way analysis of variance (ANOVA) using GraphPad Prism 8. *p-value* < 0.05 was considered statistically significant.

# Chapter 6 – Results

## 6.1 CD

### 6.1.1 Characterization

#### 6.1.1.1.Absorbance and fluorescence Spectrum

CD were characterized according to their optical properties from UV-vis absorption and the fluorescence emission spectrum. As show in **figure 6**, CD have a fluorescence maximum at wavelength about 520 nm when irradiated at 360 nm and an absorption of 360 nm. Decreasing absorption from ultraviolet to visible is typical of these CD. All fluorescence spectra were excited at 405 nm.

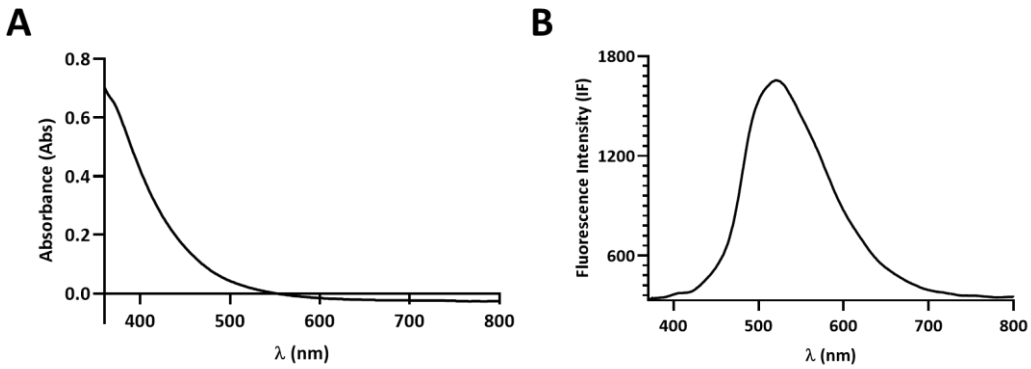


*Figure 6 - Absorbance (A) and fluorescence (B) spectrum of CD.*

After dialysis, it was observed a decrease in the fluorescence which confirmed the DEG removal from the CD mixture, as visualized in **figure 7**.

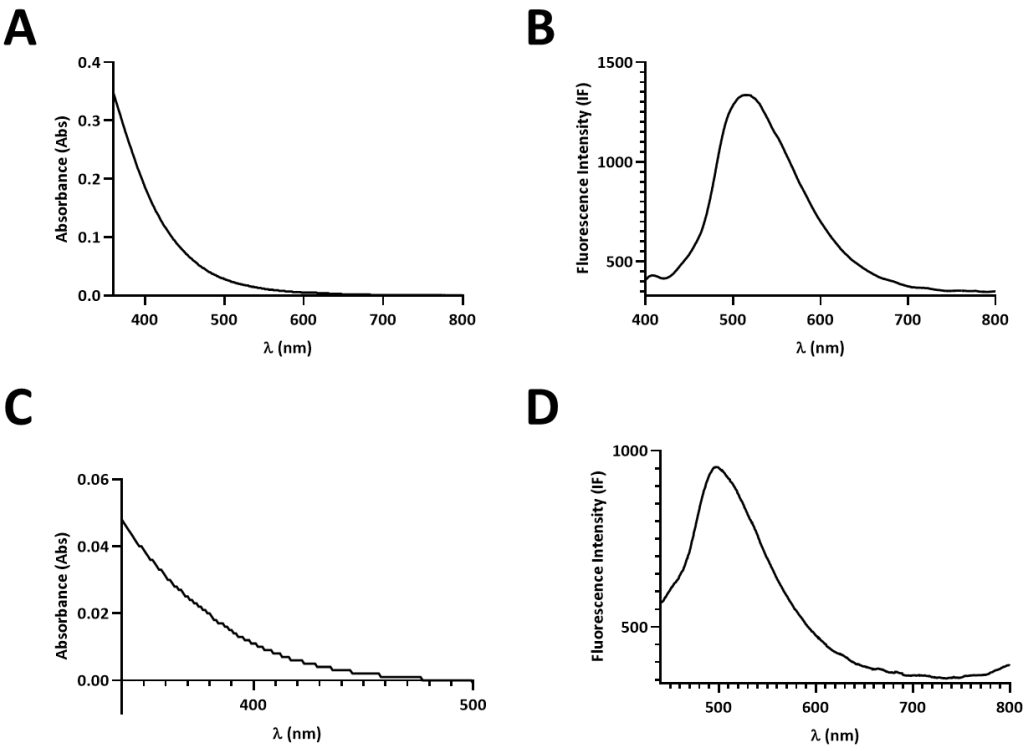


*Figure 7 - Absorbance and fluorescence spectra of CD after dialysis (CD_D) (A and B) and DEG diluted in deionized water (C and D). The same concentration of CD and DEG was used so that we could compare by fluorescence.*

Afterwards, CD underwent further purification steps which included centrifugation and filtration through a 0,22 µm filter to remove larger particles. Next, we used a 3 kDa molecular filter where the result is particles smaller than 3 kDa and with homogeneous size (**figure 8**).

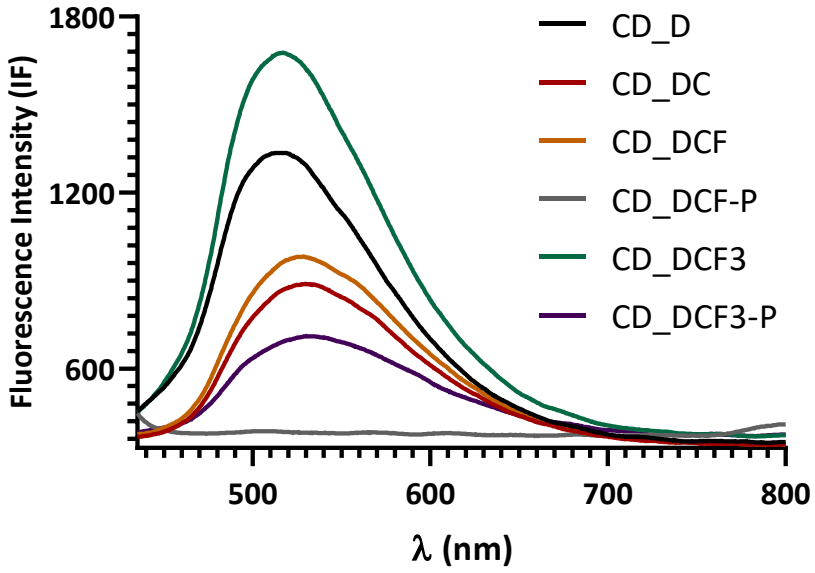


*Figure 8 - Graphical representation of CD purification steps. This schematic represents the dialysis (CD_D), after centrifugation (CD_DC) and 0,22 µm filter (CD_DCF) as well as the pellet (CD_DCF-P) and the use of the 3 kDa molecular filter (CD_DCF3) and the pellet (CD_DCF3-P).*

After all the purification process, the CD were lyophilized obtaining a caramel-like compound that was used for characterization in the different techniques such as DLS, TEM and FTIR.

### 6.1.1.2.DLS

Based on this technique, CD have a hydrodynamic diameter of less than 2 nm (**figure 9-A**) and a zeta potential ranging between -20 and 18 mV (**figure 9-B**).

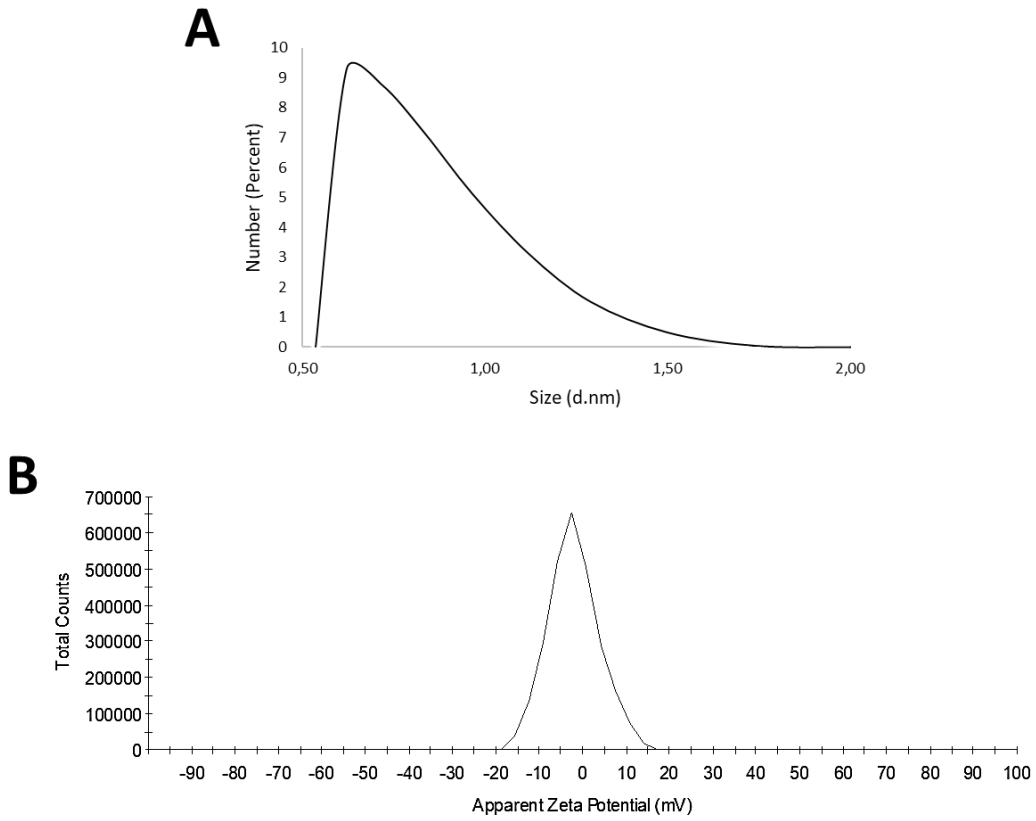


*Figure 9 - CD hydrodynamic diameter (A) and zeta potential (B).*

### 6.1.1.3.TEM

According to this technique, CD have a round morphology with a size between 2 and 6 nm and average size 3.1 ± 1.8 nm obtained by measuring 126 particles as shown in **figure 10**-**A** and **B**. In addition, by high-resolution transmission electron microscopy, it was possible to visualize the crystal structure of the CD as demonstrated in **figure 10**-**C**.

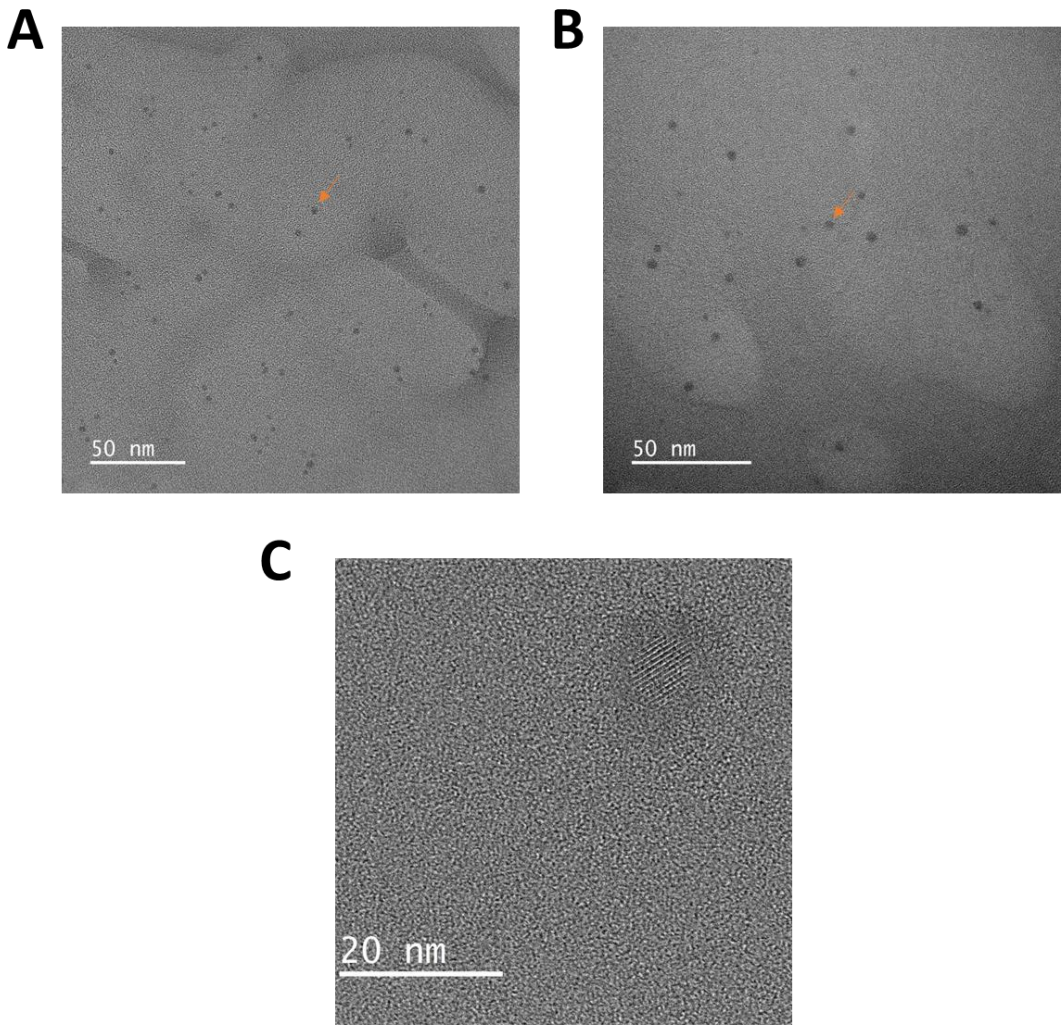


*Figure 10 - TEM images demonstrating the size and round morphology of the CD (A and B) and high-resolution transmission electron microscopy images where their crystalline structure is visualized (C). CD were highlighted with orange arrows.*

### 6.1.1.4.FTIR

Covalent bonds are known to have a change in vibrational energy due to their ability to absorb radiation at different wavelengths[67]. Infrared radiation induces a bond type that will depend on the bonding atoms[67]. For this reason, the transmittance spectrum differs depending on the molecule, since each bond and functional group absorbs at different frequencies[67]. This allows to obtain the different functional groups present in the CD (**figure 11**).

The peaks represented in the spectrum are characteristic of CD[68]. The broad band with an absorption peak at 3550-3200 represents vibrations of the stretching O-H bonds[68]. The absorption peak 3200-2700 shows O-H stretching vibrations[68]. The presence of the absorption peak 1658-1648 represents vibrations in the C=C stretching band[68]. The absorption peak 1450 shows C-H bending vibrations[68]. The peak 1390-1310 represents vibrations in O-H bending. The representative peak 1275-1200 shows vibrations in C-O bond stretching[68]. The absorption peak 1085-1050 shows vibrations in C-O bonding[68]. The peak at approximately 920 symbolizes the presence of O-H bonds. The presence of absorption peak

840-790 corresponds to vibration of C=C bond[68]. And as is characteristic of almost all organic matter, this spectrum is not elucidative of its constitution.

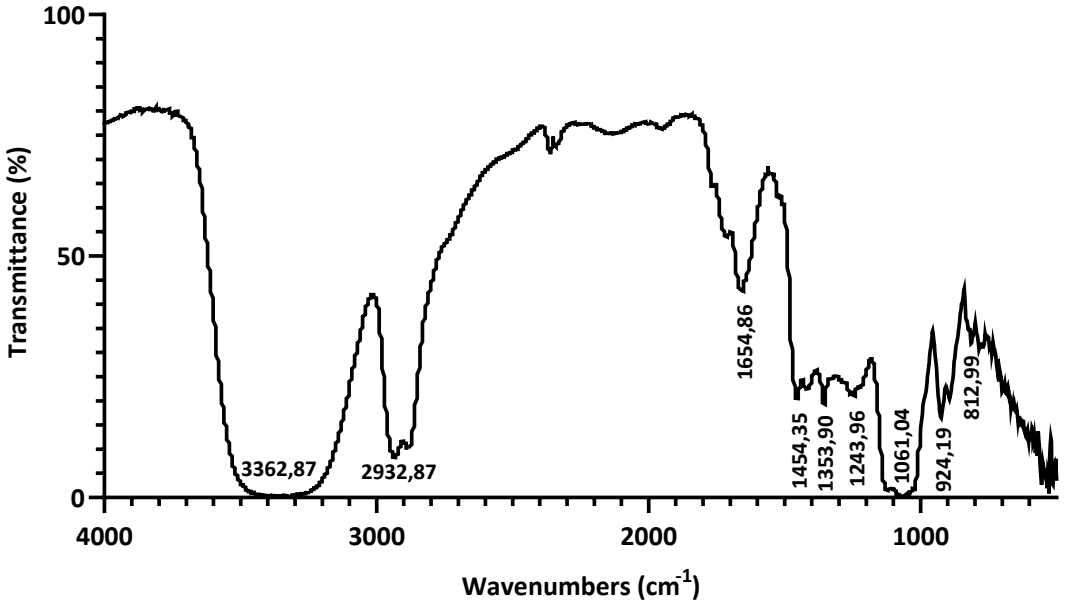


*Figure 11 - FTIR spectrum of the CD. Each absorption peak represents vibrations in a functional group, in this case characteristic CD functional groups: O-H, O-H, C=C, C-H, O-H, C-O, C-O, O-H, C=O, respectively.*

## 6.2 Cell culture

### 6.2.1 MCF-10A and BT474 cell lines

#### 6.2.1.1.Viability assay

The CD impact on cell viability was tested on MCF-10A (healthy control) and BT474 (tumor cell line) as shown in **figures 12** and **13**, respectively. Concentrations from 1 mg/mL to 10 mg/mL were tested. In BT474, CD showed an IC50 at approximately 6 mg/mL.

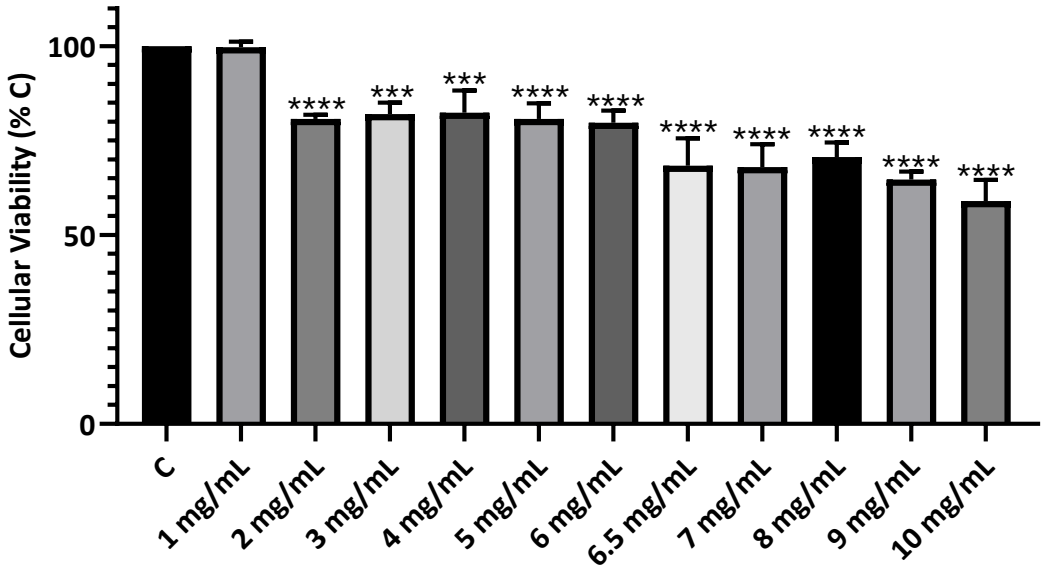


*Figure 12 - Cell viability assay of MCF-10A at different concentrations of CD. Values are statistically significant compared to the control (C), except for 1 mg/mL. ***p-value < 0.001; ****p-value < 0.0001.*

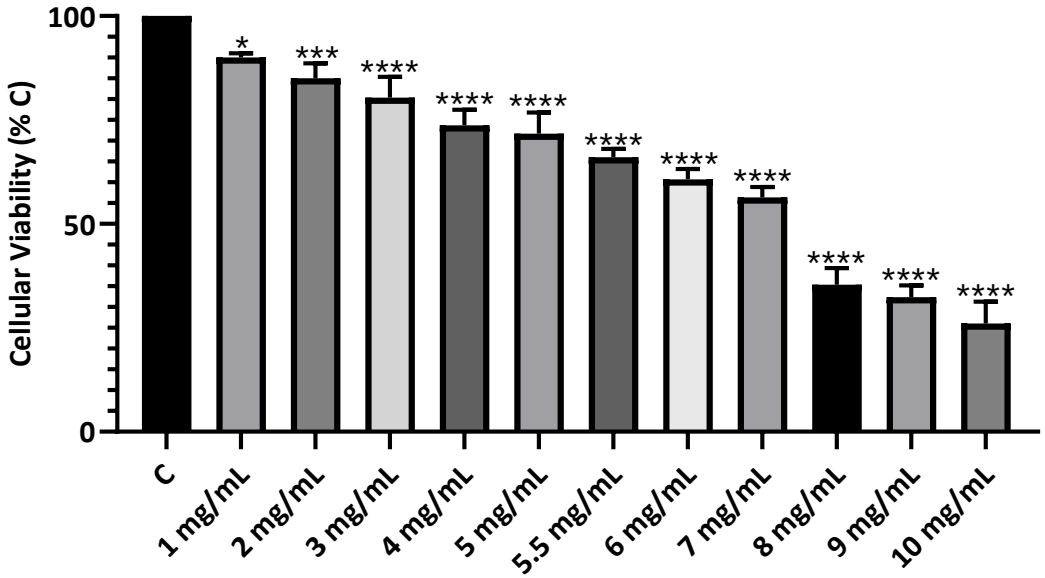


*Figure 13 - Cell viability assay of BT474 cells at different concentrations of CD. Values are statistically significant compared to the control (C). *p-value < 0.05; ***p-value < 0.001; ****p-value < 0.0001.*

### 6.2.1.2.Proliferation Assay

CD were tested on cell proliferation at concentrations close to the IC50, i.e., 5, 5.5 and 6 mg/mL, in MCF-10A and BT474 cell lines as shown in **figure 14-A** and **14-B**, respectively. It was observed a decrease in the proliferation rate in both cell lines. In MCF-10A and BT474, there was a significant increase in cell proliferation as the CD concentration increased. CD revealed a greater impact on the proliferation of tumor cells.

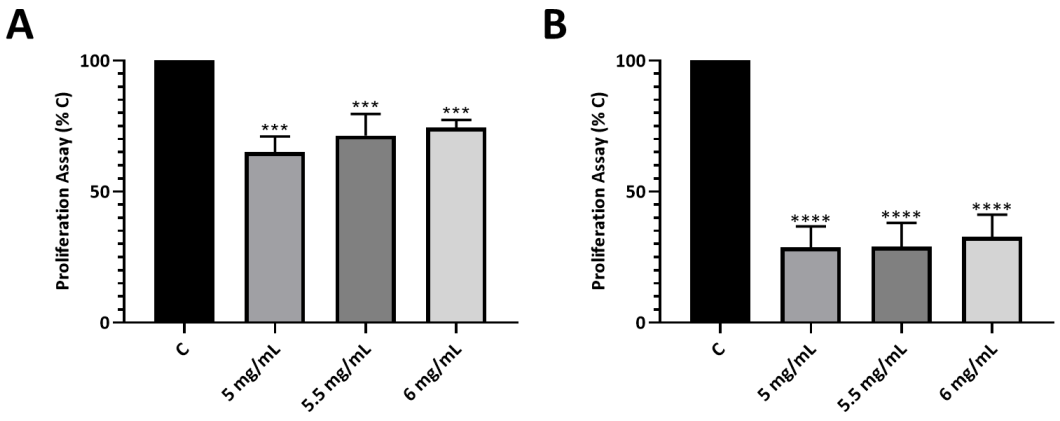


*Figure 14 - Cell proliferation assay of MCF-10A (A) and BT474 (B) cells measured at CD concentrations close to IC50. Values are statistically significant compared to control (C). ***p-value < 0.001; ****p-value < 0.0001.*

### 6.2.1.3.Injury

CD was tested on injury at concentrations close to the IC50, i.e., 5, 5.5 and 6 mg/mL, in MCF-10A and BT474 cell lines, as shown in **figures 15** and **17-A** and **figures 16** and **17-B**, respectively. CD had a greater effect on the BT474 injury, especially at 6 mg/mL where there was a reduction in damage of around 40%. MCF-10A injury remained almost intact in the presence of CD. At 5 mg/mL, the damage was repaired by around 4% and this decreased as the concentration of CD increased. There were no significant values in cell lines.

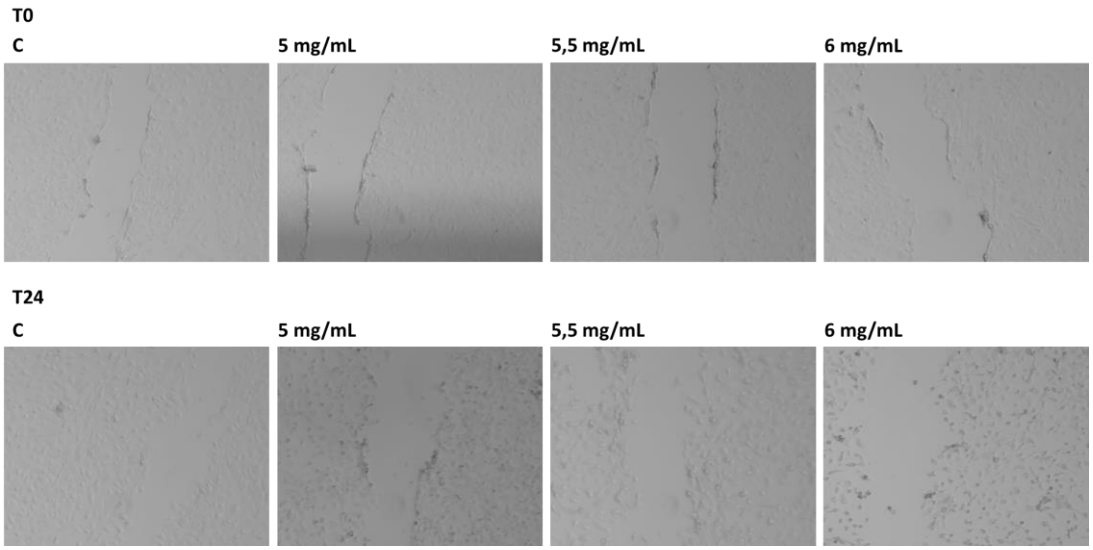


*Figure 15 - Representation of the injury assay at T0 and T24. The injury assay of MCF-10A cells was performed with CD at concentrations near the IC50.*

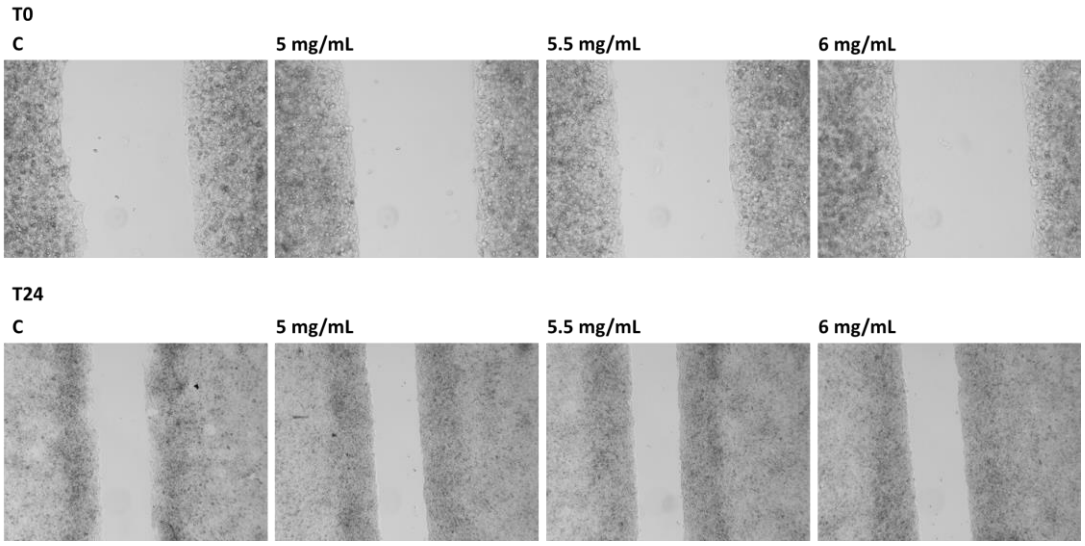


*Figure 16 - Representation of the injury assay at T0 and T24. The injury assay of BT474 cells was performed with CD at concentrations near the IC50.*

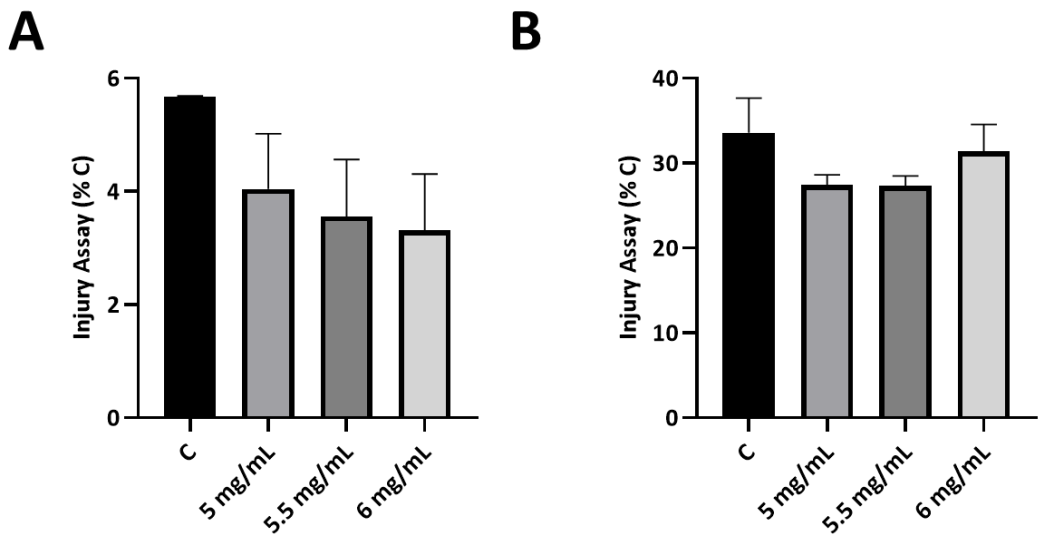


*Figure 17 - Injury assay of MCF-10A (A) and BT474 (B) cells measured at CD concentrations close to the IC50. The values are not statistically significant compared to the control (C).*

### 6.2.1.4.Migration

CD were tested on cell migration at concentrations close to the IC50, i.e., 5, 5.5 and 6 mg/mL, in MCF-10A and BT474 cell lines as shown in **figure 18-A** and **18-B**, respectively. In MCF-10A, an increase in cell migration was observed at higher concentrations of CD compared to the BT474 cell line which had a variable migration rate with greater migration at a concentration of 5.5 mg/mL. The values are statistically significant compared to the control (C), except for MCF-10A at 6 mg/mL.

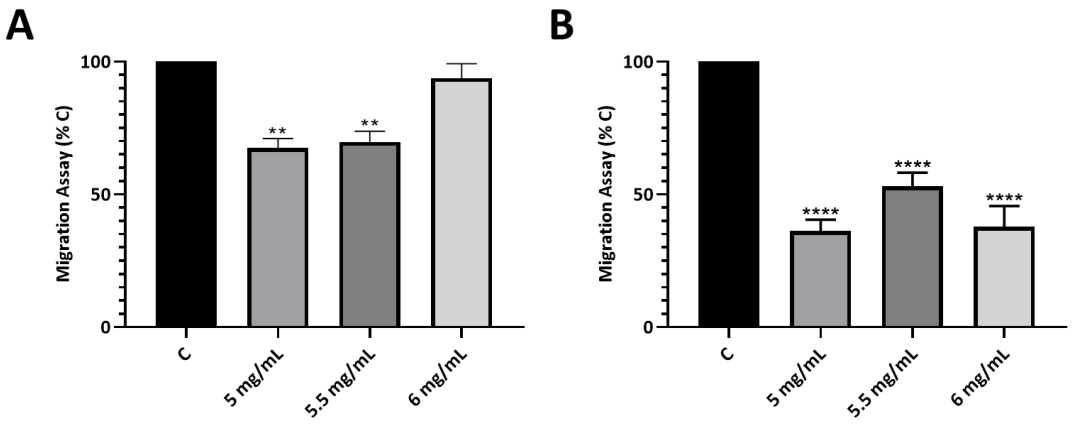


*Figure 18 - Cell migration of MCF-10A (A) and BT474 (B) measured at CD concentrations close to IC50. Values are statistically significant compared to control (C), except for 6 mg/mL in MCF-10A. **p-value < 0.01; ****p-value < 0.0001.*

## 6.3 Oxidative Stress

### 6.3.1 Antioxidant Enzymes

#### 6.3.1.1.SOD

The percentage of SOD inhibition was tested in MCF-10A and BT474 cell lines with CD at concentrations close to the IC50, i.e., 5, 5.5 and 6 mg/mL, as shown in **figure 19-A** and **19-B**, respectively. There was greater inhibition of SOD in MCF-10A. No statistical significance was achieved in both cell lines.

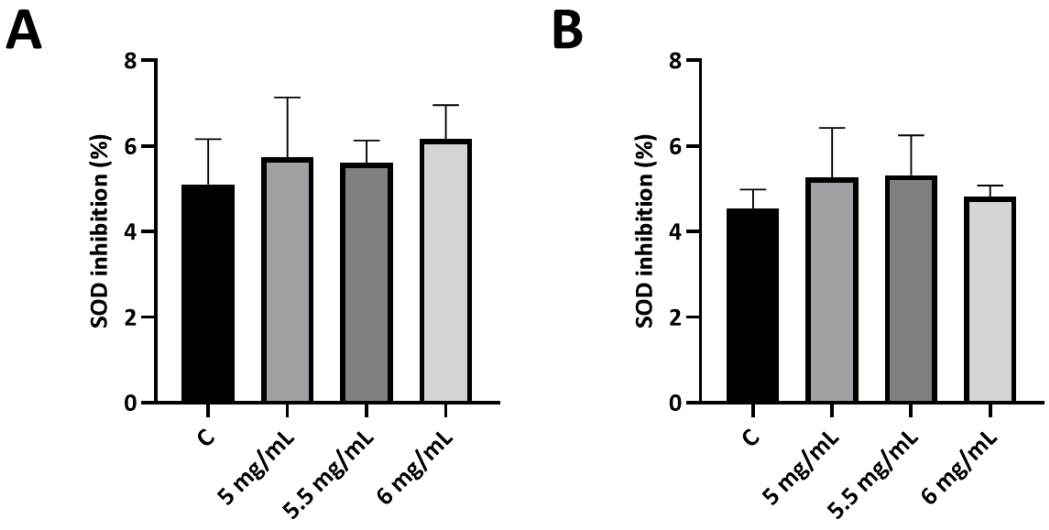


*Figure 19 - Percentage of SOD inhibition in MCF-10A (A) and BT474 (B) cell lines measured at CD concentrations close to IC50. The values are not statistically significant compared to the control (C).*

#### 6.3.1.2.Catalase

Catalase activity was tested in MCF-10A and BT474 cell lines with CD at concentrations close to the IC50, i.e., 5, 5.5 and 6 mg/mL, as illustrated in **figure 20-A** and **20-B**, respectively. Catalase activity was lower in BT474 when compared to MCF-10A. In the treatment conditions no statistical difference was observed.

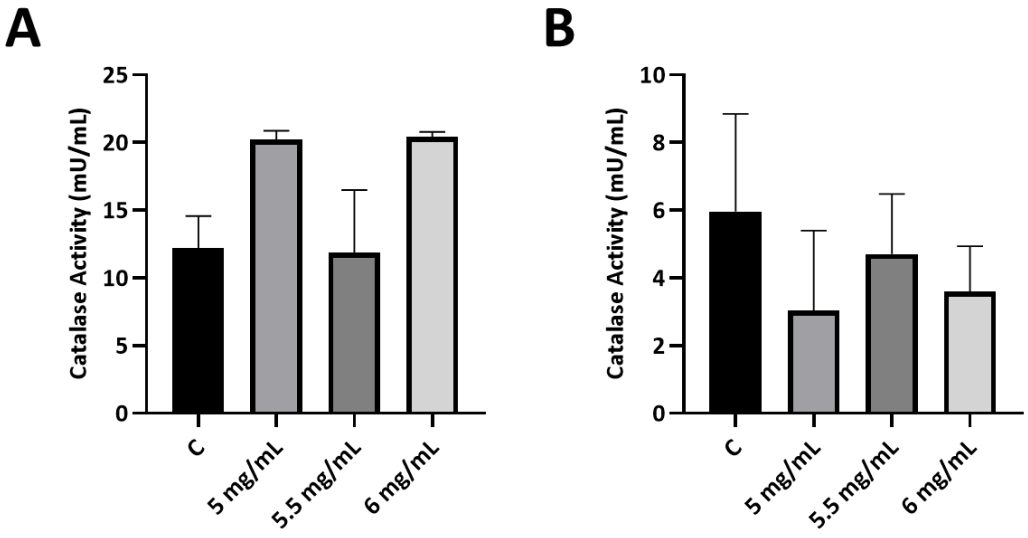


*Figure 20 - Catalase activity (mU/mL) in MCF-10A (A) and BT474 (B) cell lines measured at CD concentrations close to IC50. The values are not statistically significant compared to the control (C).*

### 6.3.1.3.GSH

GSH was tested in MCF-10A and BT474 cell lines with CD at concentrations close to the IC50, i.e., 5, 5.5 and 6 mg/mL, as seen in **figure 21-A** and **21-B**, respectively. There are higher GSH values in BT474, except at a concentration of 6 mg/mL, without significant values in any cell line.

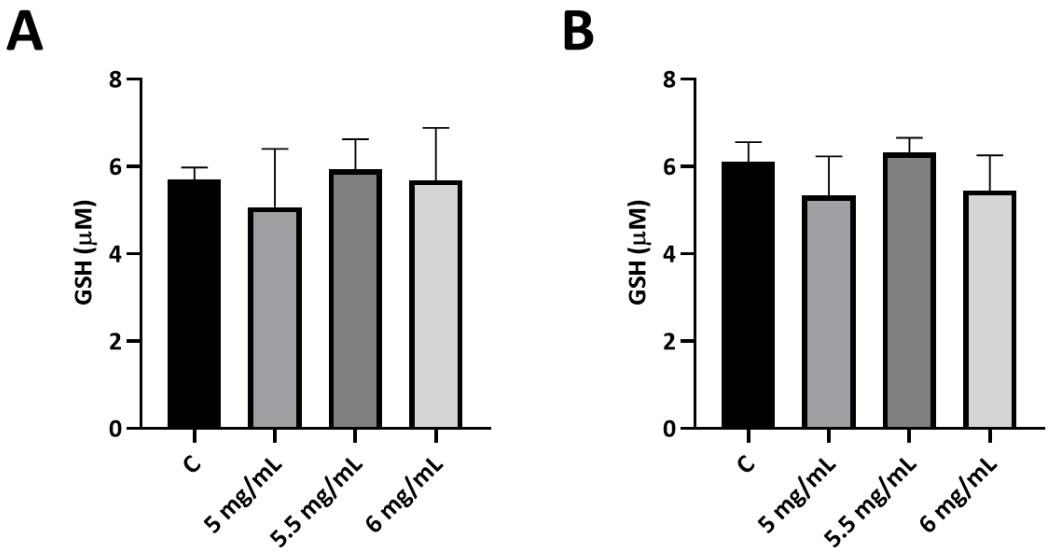


*Figure 21 - GSH (μM) in MCF-10A (A) and BT474 (B) cell lines measured at CD concentrations close to the IC50. The values are not statistically significant compared to the control (C).*

## 6.3.2 Antioxidant Activity

### 6.3.2.1.DPPH

DPPH activity was tested on the MCF-10A and BT474 cell lines with CD at concentrations close to the IC50, i.e., 5, 5.5 and 6 mg/mL, as shown in **figure 22-A** and **22-B**. The antioxidant activity was found to be higher in BT474 cells. All values are statistically significant.

DPPH activity of CD with MCF-10A and BT474 culture medium and water was also assessed at concentrations close to the IC50, as shown in **figure 23-A, B** and **C**, respectively. It was found that the antioxidant activity of CD was higher when diluted with BT474 culture medium. There are no significant values.

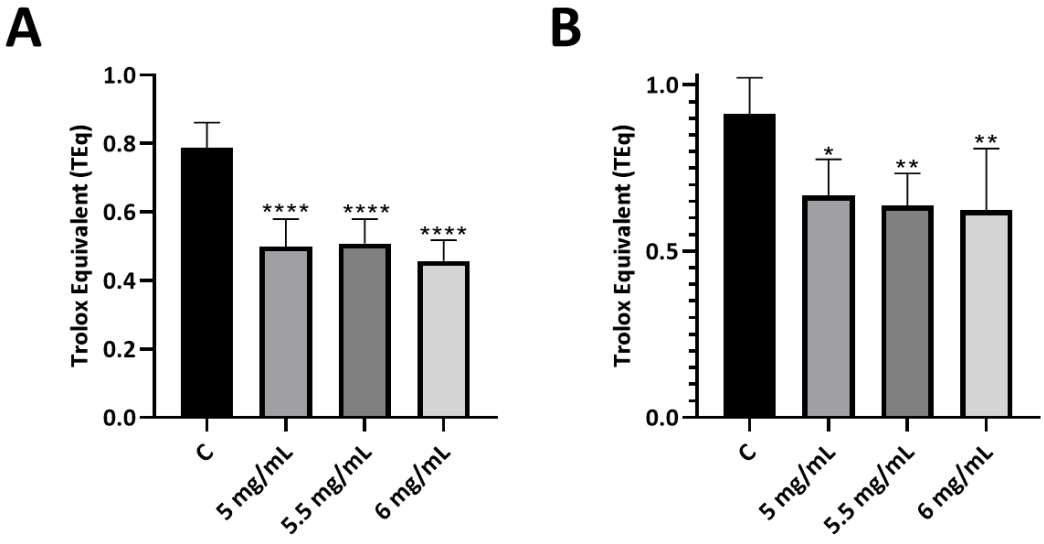


*Figure 22 - DPPH activity (TEq) in MCF-10A (A) and BT474 (B) cell lines measured at CD concentrations close to the IC50. The values are statistically significant compared to the control (C). *p-value < 0.05; **p-value < 0.01; ****p-value < 0.0001.*

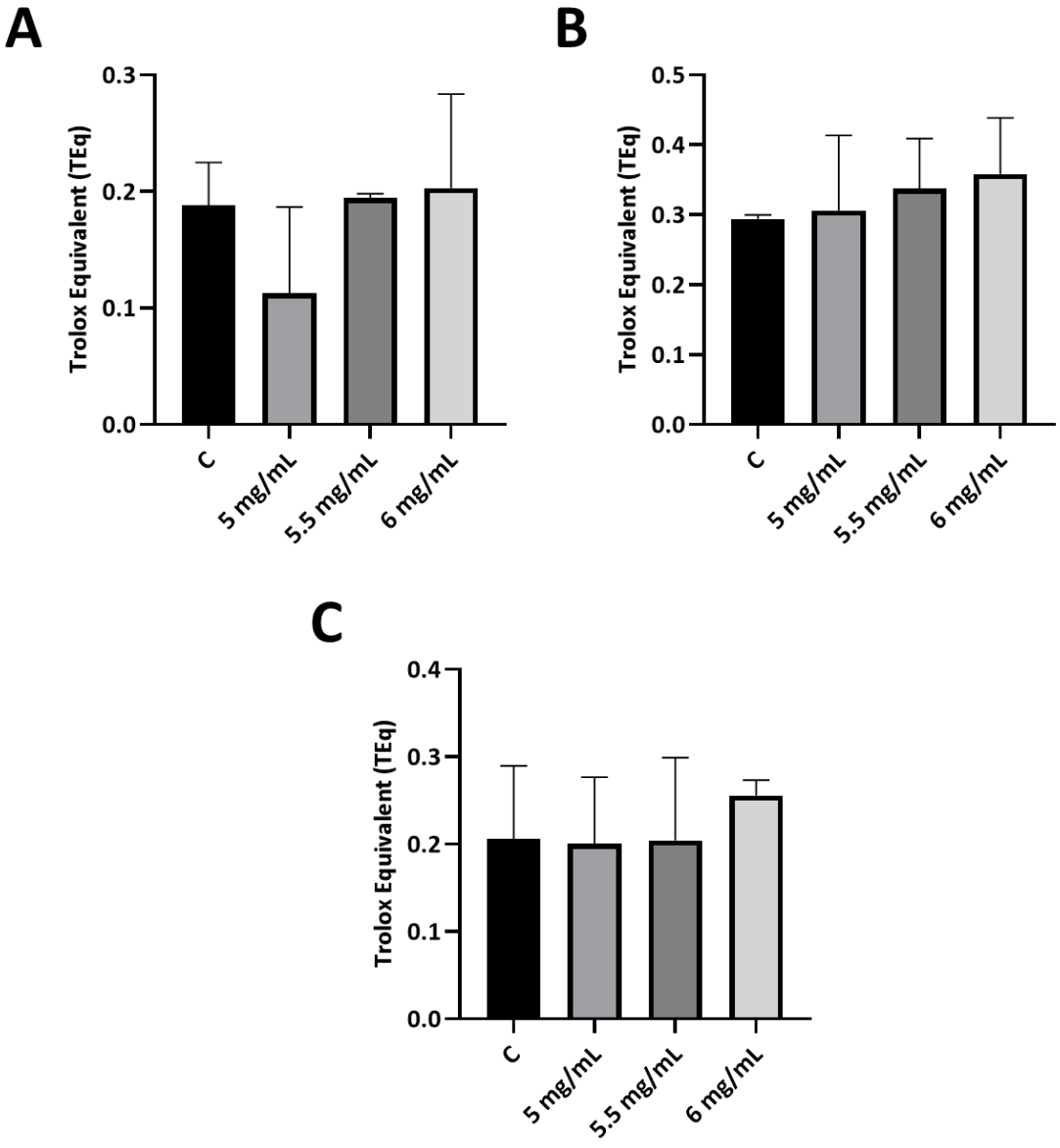


*Figure 23 - DPPH activity (TEq) in CD diluted in MCF-10A (A) and BT474 (B) culture medium and water (C) at concentrations close to the IC50. The values are not statistically significant compared to the control (C).*

# 6.4 Cytotoxicity Assay

## 6.4.1 Intracellular Enzyme

### 6.4.1.1.LDH

Total LDH was tested in MCF-10A and BT474 cell lines with CD at concentrations close to the IC50, i.e., 5, 5.5 and 6 mg/mL, as indicated in **figure 24-A** and **24-B**, respectively. Total LDH released into the extracellular environment was found to be higher in MCF-10A cells, except in control. There were no significant values in any cell line.

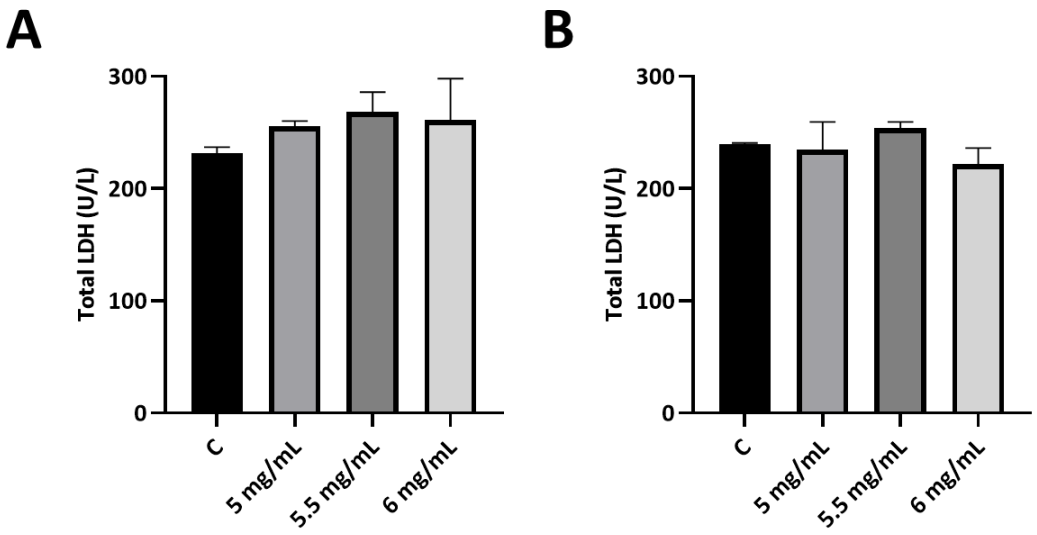


*Figure 24 - Total LDH (U/L) in MCF-10A (A) and BT474 (B) cell lines measured at CD concentrations close to IC50. The values are not statistically significant compared to the control (C).*

# Chapter 7 – Discussion

CD have been widely applied for use in biomedicine especially for their small size, fluorescence, low cytotoxicity and high incorporation rate in biological systems.

In this study, we used fructose-derived CD as potential onco-therapeutics for breast cancer. Fructose-derived CD were synthesized from microwave irradiation by the bottom-up method. To the best of our knowledge, using fructose as the carbon source is a pioneer study. D-fructose is a monosaccharide that contains 6 carbons and a keto group which allows to be a reducing sugar. It is more soluble in water than other sugars. A study revealed that fructose alone increases the adhesion of tumor cells to active endothelial cells, increases the migration of tumor cells, intervenes in tumor invasion and alters the shape and size of tumor cells causing them to lose contact with neighboring cells[69].

CD existence was confirmed by the fluorescence spectrum obtained with a broad band. Fluorescence is the key point and the reason why CD have been so widely investigated in recent times due to their use in cellular imaging which makes it possible to detect and visualize tumor cells and thus make a diagnosis.

CD underwent purification processes including dialysis, centrifugation, filtration (use of a 0.2 µm filter and a 3 kDa molecular filter) and lyophilization. Dialysis led to the removal of the organic solvent (DEG), as result, it was observed a decrease in the fluorescence spectrum of the CD compared to the original CD fluorescence The DEG acts as a precursor for the CD and is essential in the syntheses process. By removing DEG, it is assured that results on the cell-based assays are result of the CD.

After centrifugation and the use of the 0,22 µm filter we also found a decrease in fluorescence, confirming the CD purification. Agglomerates and impurities were considered removed by these methods.

To homogenize the size of the CD, we used a 3 kDa filter. As a result, it was obtained particles smaller than the pore size of the filter. Higher fluorescence confirmed the CD purity and homogeneity.

To finish the purification processes, we lyophilized the CD in order to obtain a caramel like-compound and thus facilitate handling both in the further techniques and in the cellular-based assays. We obtained a caramel-like compound that was expected due to the caramelization process involved in the formation of the CD. The process of caramelization is the formation of caramel from the heat treatment of sugar. CD that uses sugars as a carbon source and are synthesized at high temperatures undergo the caramelization process. This process leads to the dehydration of the sugar and can cause chemical reactions such as oxidation, condensation and polymerization, the formation of intramolecular covalent bonds and rearrangements in the structure[70].

From the characterization techniques, it was possible to profile the CD according to their size, morphology, structure, functional groups and fluorescence.

According to TEM, CD are round, have a crystalline structure and the size ranges between 2 and 6 nm with an average particle size of 3.1 ± 1.8 nm by measuring 126 particles. These results

are characteristic for CD. In general, nanoparticles are spheres composed of carbon and their size can vary between 2 and 100 nm. The presence of a crystalline structure can be justified by the fact that carbons can easily aggregate, from covalent bonds that are quite strong, which allows the formation of perfect structures. This technique confirmed the presence of CD by their visualization and characteristics.

DLS made it possible to characterize the hydrodynamic diameter of the particles, hypothetically compared to a perfect solid sphere with the same hydrodynamic friction and the zeta potential which indicates the charge of the particles. The synthesized CD have a hydrodynamic diameter smaller than 2 nm and a zeta potential between -20 and 18 mV. The results were expected since we obtain small diameters and a more negative than positive charge that can be explained by the presence of carbonyl and carboxyl groups.

The FTIR technique, which allows the functional groups to be obtained by comparing bands in the infrared spectrum, demonstrated the presence of the O-H, C=C, C-H, C-O and C=O functional groups. This demonstrates that fructose-derived CD are composed of carbon, oxygen and hydrogen. These results are characteristic of CD, according to previously described studies.

Studies have revealed similar characteristics of fructose-derived CD synthesized by the same method. CD synthesized with folic acid and urea revealed that they had a size between 1 and 7 nm and some similar molecular interactions such as C=O, C=C and O-H. Also exhibited a maximum fluorescence and absorption peak at 460 nm and 380 nm, respectively. CD synthesized from citric acid and ethylenediamine had a size between 2 and 6 nm with an average size of 3.5 nm, a maximum absorption peak of 360 nm and fluorescence of 440 nm. CD synthesized with wool showed that the size was between 1.5 and 4.5 nm with an average size of 2.8 nm and the maximum absorption and fluorescence peak was 270 nm and 365 nm, respectively[71–73].

According to these characterizations, we realized that CD have variable size as well as absorption and fluorescence spectra. CD can be synthesized for different functionalities which allows changing their properties and characteristics. The carbon source and the synthesis method are key factors to change the properties of CD.

On the other hand, we assessed CD at different concentrations (1 to 10 mg/mL) and evaluated toxicity, proliferation, migration, injury, oxidative stress and cytotoxicity in mammary epithelial line (healthy control), MCF-10A and BT474 mammary tumor cell line ($ER^+$, $PR^+$ and $HER2^+$).

Regarding cellular toxicity, CD showed a higher toxicity effect in tumor cells then in epithelial cells, nonetheless it was also observed a significant toxicity in epithelial cells. Viability decrease was constant in BT474, not observed in MCF-10A. In MCF-10A cell line, viability remained approximately constant in concentration of 2 mg/mL and higher. While in BT474 cells there is a decrease in viability when the concentration of CD increased.

Concerning cell proliferation, CD exhibit a significantly higher impact in the proliferation rate of epithelial cells when compared to tumor cells. These results are consistent with the viability results. In terms of the cell migration assay, CD revealed a greater significant effect on tumor cells than epithelial cells. In the injury assay, CD demonstrated a greater effect on tumor cell. One study showed that CD synthesized by microwave irradiation at different concentrations had

varying toxicity in MCF-10A cells[74]. In contrast, another study showed that silver CD exhibited greater cytotoxicity at lower concentrations compared to the CD in our study[75]. Another study showed that silver CD showed some toxicity in MCF-10A cells at lower concentrations than those in our study[76].

Tumor cells are known by their high metabolic rate due to the associative proliferation needs. Which in turn results in the high mitochondrial activity. Tumor cells are described to use mitochondria as an energy source for the anabolic production of biosynthesis of nucleotides, lipids and proteins to sustain their proliferation[77]. In addition, the activity of endocytosis (a cellular process that occurs vesicular membrane transport between the plasma membrane and the cytoplasmic membrane and within the intracellular membrane) increases sustained proliferation, invasion capacity and prevention of apoptosis[78].

The initial study would be to functionalize CD with drugs already used in clinical practice and evaluate their antitumor effect in a cell line with positive and another with negative expression of all receptors (ER, PR and HER2). As the BT474 cell line has positive expression of all receptors, it would be a promising target to evaluate the antitumor effect of functionalized CD. However, we were unable to perform functionalization and therefore tested fructose-derived CD on the BT474 line with all positive receptors.

Studies have shown that CD interact with the cytoplasm and organelles namely mitochondria among others via endocytosis[79,80].

Tumor cells have an extreme capacity for angiogenesis which favors cell proliferation, invasion, metastasis and resistance to cell apoptosis[81]. They progress at high levels of ROS, so the activity of antioxidant enzymes is reduced[58]. Cells exposed to high levels of oxidative stress suffer damage at the level of proteins, nucleic acids, lipids, membranes and organelles which can trigger the activation of cell death processes such as apoptosis[82]. Apoptosis can be induced from 3 pathways: mitochondria, endoplasmic reticulum and death receptor[80].

Studies point that apoptosis induced by mitochondria can be promoted by CD. CD generate ROS which affects the mitochondrial pathway causing stress and increased mitochondrial membrane permeability. With the increased permeability, cytochrome C is released into the cytosol and converted into a complex that is composed of apoptosis activating factor-1 (APAF-1) and procaspase-9. This leads to the stimulation of caspase-9 which activates the apoptosis executors. On the other hand, the effect of CD leads to decreased levels of heat shock protein (HSP90) which is a protein that competes with cytochrome C in the cytosol to form a complex with APAF-1 (HSP90-APAF-1). CD, by inhibiting HSP90, allow for greater cell apoptosis in tumor cells from the formation of cytochrome C with APAF-1[80].

In terms of oxidative stress assays, tumor cells are known to proliferate at high levels of ROS, increased presence of free radicals, which complicates the function of antioxidant enzymes. The main function of antioxidant enzymes is to maintain cellular homeostasis of ROS. We further quantified the expression of three key antioxidant enzymes. The role of CD in antioxidant enzymes is not yet well defined. It is only known that CD can be antioxidants and pro-oxidants.

SOD is an enzyme whose main function is to transform hydrogen superoxide into hydrogen peroxide and oxygen, preventing the formation of free radicals. Hydrogen superoxide formed

by xanthone and xanthone dismutase reacts with I.N.T (2-(4-iodophenyl)-3-(4-nitrophenol)-5-phenyltetrazolium chloride) and generates formazan dye. From the assay performed, it was found that there is a decreased inhibition of this reaction in tumor cells, which means that there is greater formation of formazan dye and less SOD activity. In epithelial cells there is a higher SOD activity due to the greater inhibition of the reaction, without significant results.

Catalase is also an antioxidant enzyme that converts hydrogen peroxide into oxygen and water. In the assay performed we evaluated the activity of catalase by the amount of hydrogen peroxide that was not converted. We found that catalase activity is lower in tumor cells.

SOD and catalase activity is lower in tumor cells which demonstrates higher levels of free radicals in these cells. In tumor cells these two antioxidant enzymes should have higher activity to maintain the redox balance.

In addition, reduced SOD activity is associated with decreased cell survival from aerobic mechanisms. The relationship between intracellular superoxide and hydrogen peroxide is known to play a central role in cell fate. Increased levels of superoxide and decreased levels of hydrogen peroxide leads to apoptosis inhibition and cell survival. While in opposite levels, there is activation of cell apoptosis by caspase proteases. In addition, lower SOD activity leads to increased toxicity by hydrogen peroxide and thus may lead to further cell damage[83,84].

Regarding total glutathione, it was found to be increased in tumor cells, except at 6 mg/mL. Glutathione levels were expected to be higher at higher CD. At higher CD concentration, due to possible mitochondrial dysfunction, total glutathione may decrease. Glutathione is known to be associated with the mitochondrial enzyme GPX4. High levels of ROS can lead to glutathione depletion and in turn interrupt the pathway which after being interrupted by glutathione depletion can lead to lipid peroxidation and in turn cell death. In addition, high levels of glutathione are essential for tumor formation and proliferation.

CD may have an impact on the accumulation of damage in mitochondria in tumor cells by the formation of ROS. Mitochondria under conditions of oxidative stress from high levels of ROS may be less efficient at communicating to defense mechanisms. That is, due to the inability of mitochondria to protect cells from high levels of ROS, damage may occur to mitochondrial DNA, proteins and lipids. It can also cause permeability in the mitochondrial membrane and disturbances in $Ca^{2+}$ homeostasis. All of this can lead to ongoing oxidative stress that antioxidant enzymes are unable to combat[85].

However, if CD causes apoptosis of the mitochondria of the tumor cells and, as a result, there is a reduction in the ROS present in the microenvironment, there may be a reduction in the activity of the antioxidant enzymes. As well as LDH activity, since tumor cells progress more easily using anaerobic mechanisms that are more productive in terms of energy for tumor survival. As CD has an antitumor effect, decreasing cell proliferation and increasing toxicity, it can lead to a decrease in the use of LDH for energy production.

Our results revealed that CD may not interfere with cellular assays via oxidative stress pathways. Since the results were controversial, that is, the activity of the antioxidant enzymes SOD and catalase was lower in tumor cells while total glutathione was higher. In addition, there

is higher LDH on the outside of MCF-10A cells. And the antioxidant power measured by DPPH assay is greater in the tumor cells.

# Chapter 8 – Conclusion

The fructose-derived CD were synthesized and characterized according to their size, morphology, structure, fluorescence and functional groups. As expected, fructose-derived CD are composed of carbon, oxygen and hydrogen. As is also characteristic of CD, they are fluorescent with an absorption spectrum of 360 nm and an emission spectrum with a broad emission band around 520 nm. They have a round morphology with sizes between 2 and 6 nm (average particle size 3.1 ± 1.8 nm), a hydrodynamic diameter of less than 2 nm and a crystalline structure.

These CD showed antitumor capability, although with significant toxicity in epithelial cells. Which demonstrates their onco-therapeutic effect for breast cancer.

Regarding oxidative stress, the results reveal that the influence of CD on cellular tests may not be based on oxidative stress pathways.

# Chapter 9 – Future Perspectives

Cancer treatments such as chemotherapy and radiotherapy are known to affect tumor cells to a great extent. However, it is also known that epithelial cells suffer significant damage that can trigger severe systemic damage.

CD have the advantage to be functionalize with other compounds. Studies have shown that functionalized CD demonstrate lower side effects and higher targeting accuracy in tumor cells, relieving normal cells.

One potential solution is the functionalization of CD with the anti-tumoral drugs. The future perspective of this work includes the functionalization of CD with anti-tumoral drugs in order to targeted tumor cells and decrease toxicity in normal cells. The use of BT474 cell line (positive for all receptors) will allow the functionalization of compounds used in endocrine therapy as well as compounds used in HER2 enriched BC. Moreover, lower concentrations of CD could be used to obtain the same tumor toxicity with functionalized CD.

# Chapter 10 – References


1. Nocito G, Calabrese G, Forte S, et al. Carbon dots as promising tools for cancer diagnosis and therapy. *Cancers (Basel)*. 2021;13(9):1-14. doi:10.3390/cancers13091991

2. Sharma A, Das J. Small molecules derived carbon dots: synthesis and applications in sensing, catalysis, imaging, and biomedicine. *Journal of Nanobiotechnology 2019 17:1*. 2019;17(1):1-24. doi:10.1186/S12951-019-0525-8

3. Deo SVS, Sharma J, Kumar S. GLOBOCAN 2020 Report on Global Cancer Burden: Challenges and Opportunities for Surgical Oncologists. *Ann Surg Oncol*. 2022;29(11):6497-6500. doi:10.1245/S10434-022-12151-6/METRICS

4. Wareing TC, Gentile P, Phan AN. Biomass-Based Carbon Dots: Current Development and Future Perspectives. *ACS Nano*. 2021;15(10):15471-15501. doi:10.1021/ACSNANO.1C03886/ASSET/IMAGES/LARGE/NN1C03886_0011.JPEG

5. Malavika JP, Shobana C, Sundarraj S, Ganeshbabu M, Kumar P, Selvan RK. Green synthesis of multifunctional carbon quantum dots: An approach in cancer theranostics. *Biomaterials Advances*. 2022;136:212756. doi:10.1016/J.BIOADV.2022.212756

6. Yi C, Pan Y, Fang Y. *Chapter 5 - Surface Engineering of Carbon Nanodots (C-Dots) for Biomedical Applications*. Elsevier Inc.; 2019. doi:10.1016/B978-0-12-814497-8.00005-9

7. Jia Y, Chen S, Wang C, Sun T, Yang L. Hyaluronic acid-based nano drug delivery systems for breast cancer treatment: Recent advances. *Front Bioeng Biotechnol*. 2022;10. doi:10.3389/fbioe.2022.990145

8. Wang Y, Li X, Zhao S, et al. Synthesis strategies, luminescence mechanisms, and biomedical applications of near-infrared fluorescent carbon dots. *Coord Chem Rev*. 2022;470:214703. doi:10.1016/J.CCR.2022.214703

9. Mansuriya BD, Altintas Z. Carbon dots: Classification, properties, synthesis, characterization, and applications in health care-an updated review (2018–2021). *Nanomaterials*. 2021;11(10). doi:10.3390/nano11102525

10. Xia C, Zhu S, Feng T, Yang M, Yang B. Evolution and Synthesis of Carbon Dots: From Carbon Dots to Carbonized Polymer Dots. *Advanced Science*. 2019;6(23):1901316. doi:10.1002/ADVS.201901316

11. Gupta V, Bhavanasi S, Quadir M, et al. Protein PEGylation for cancer therapy: bench to bedside. *J Cell Commun Signal*. 2019;13(3):319-330. doi:10.1007/s12079-018-0492-0

12. Yang F, He Q, Dai X, Zhang X, Song D. The potential role of nanomedicine in the treatment of breast cancer to overcome the obstacles of current therapies. *Front Pharmacol*. 2023;14. doi:10.3389/fphar.2023.1143102

13. Liu J, Li R, Yang B. Carbon Dots: A New Type of Carbon-Based Nanomaterial with Wide Applications. *ACS Cent Sci*. 2020;6(12):2179-2195. doi:10.1021/ACSCENTSCI.0C01306/ASSET/IMAGES/LARGE/OC0C01306_0007.JPEG

14. Rossini EL, Milani MI, Pezza HR. Green synthesis of fluorescent carbon dots for determination of glucose in biofluids using a paper platform. *Talanta*. 2019;201:503-510. doi:10.1016/J.TALANTA.2019.04.045

15. De B. Carbon Dots and Their Polymeric Nanocomposites. *Nanomaterials and Polymer Nanocomposites: Raw Materials to Applications*. Published online January 1, 2019:217-260. doi:10.1016/B978-0-12-814615-6.00007-2

16. Cohen EN, Kondiah PPD, Choonara YE, du Toit LC, Pillay V. Carbon Dots as Nanotherapeutics for Biomedical Application. *Curr Pharm Des*. 2020;26(19):2207-2221. doi:10.2174/1381612826666200402102308

17. Khayal A, Dawane V, Amin MA, et al. polymers Advances in the Methods for the Synthesis of Carbon Dots and Their Emerging Applications. Published online 2021. doi:10.3390/polym13183190

18. Chen B Bin, Huang CZ. Preparation of carbon dots and their sensing applications. *Sensing and Biosensing with Optically Active Nanomaterials*. Published online January 1, 2022:9-40. doi:10.1016/B978-0-323-90244-1.00005-7

19. Liu ML, Chen B Bin, Li CM, Huang CZ. Carbon dots: synthesis, formation mechanism, fluorescence origin and sensing applications. *Green Chemistry*. 2019;21(3):449-471. doi:10.1039/C8GC02736F

20. Yang HL, Bai LF, Geng ZR, et al. Carbon quantum dots: Preparation, optical properties, and biomedical applications. *Mater Today Adv*. 2023;18:100376. doi:10.1016/J.MTADV.2023.100376

21. Stephenson FH. Centrifugation. In: *Calculations for Molecular Biology and Biotechnology*. Elsevier; 2016:431-438. doi:10.1016/B978-0-12-802211-5.00012-6

22. Fong JFY, Ng YH, Ng SM. Carbon dots as a new class of light emitters for biomedical diagnostics and therapeutic applications. *Fullerenes, Graphenes and Nanotubes: A Pharmaceutical Approach*. Published online January 1, 2018:227-295. doi:10.1016/B978-0-12-813691-1.00007-5

23. Berg John L Tymoczko Lubert Stryer with Gregory J Gatto JM, H Freeman JW, York Biochemistry N. *SEVENTH EDITION*.

24. Tian X, Yin X. Carbon Dots, Unconventional Preparation Strategies, and Applications Beyond Photoluminescence. *Small*. 2019;15(48):1901803. doi:10.1002/smll.201901803

25. Cui L, Ren X, Sun M, Liu H, Xia L. Carbon Dots: Synthesis, Properties and Applications. *Nanomaterials*. 2021;11(12). doi:10.3390/NANO11123419

26. Li Z, Wang L, Li Y, Feng Y, Feng W. Frontiers in carbon dots: design, properties and applications. *Mater Chem Front*. 2019;3(12):2571-2601. doi:10.1039/C9QM00415G

27. Seidu TA, Kutoka PT, Asante DO, Farooq MA, Alolga RN, Bo W. Functionalization of Nanoparticulate Drug Delivery Systems and Its Influence in Cancer Therapy. *Pharmaceutics*. 2022;14(5). doi:10.3390/pharmaceutics14051113

28. Yi C, Pan Y, Fang Y. *Surface Engineering of Carbon Nanodots (C-Dots) for Biomedical Applications*. Elsevier Inc.; 2019. doi:10.1016/B978-0-12-814497-8.00005-9

29. Mao K, Zhang W, Yu L, Yu Y, Liu H, Zhang X. Transferrin-Decorated Protein-Lipid Hybrid Nanoparticle Efficiently Delivers Cisplatin and Docetaxel for Targeted Lung Cancer Treatment. *Drug Des Devel Ther*. 2021;15:3475. doi:10.2147/DDDT.S296253

30. Ge G, Li L, Wang D, et al. Carbon dots: synthesis, properties and biomedical applications. *J Mater Chem B*. 2021;9(33):6553-6575. doi:10.1039/D1TB01077H

31. Vieira IRS, Tessaro L, Lima AKO, Velloso IPS, Conte-Junior CA. Recent Progress in Nanotechnology Improving the Therapeutic Potential of Polyphenols for Cancer. *Nutrients 2023, Vol 15, Page 3136*. 2023;15(14):3136. doi:10.3390/NU15143136

32. Han J, Hong J, Lee H, et al. Advances in polyphenol-based carbon dots for biomedical engineering applications. *Eur Polym J*. 2023;197:112354. doi:10.1016/J.EURPOLYMJ.2023.112354

33. Naik K, Chaudhary S, Ye L, Parmar AS. A Strategic Review on Carbon Quantum Dots for Cancer-Diagnostics and Treatment. *Front Bioeng Biotechnol*. 2022;10:701. doi:10.3389/FBIOE.2022.882100/BIBTEX

34. Sharma A, Das J. Small molecules derived carbon dots: Synthesis and applications in sensing, catalysis, imaging, and biomedicine. *J Nanobiotechnology*. 2019;17(1). doi:10.1186/s12951-019-0525-8

35. Smolarz B, Zadrożna Nowak A, Romanowicz H. Breast Cancer—Epidemiology, Classification, Pathogenesis and Treatment (Review of Literature). *Cancers (Basel)*. 2022;14(10). doi:10.3390/CANCERS14102569

36. Łukasiewicz S, Czeczelewski M, Forma A, Baj J, Sitarz R, Stanisławek A. Breast Cancer—Epidemiology, Risk Factors, Classification, Prognostic Markers, and Current Treatment Strategies—An Updated Review. *Cancers (Basel)*. 2021;13(17). doi:10.3390/CANCERS13174287

37. Dass SA, Tan KL, Rajan RS, et al. Triple Negative Breast Cancer: A Review of Present and Future Diagnostic Modalities. *Medicina (B Aires)*. 2021;57(1):1-18. doi:10.3390/MEDICINA57010062

38. Bhushan A, Gonsalves A, Menon JU. Current State of Breast Cancer Diagnosis, Treatment, and Theranostics. *Pharmaceutics*. 2021;13(5). doi:10.3390/PHARMACEUTICS13050723

39. Wang Z, Liu L, Li Y, et al. Analysis of CK5/6 and EGFR and Its Effect on Prognosis of Triple Negative Breast Cancer. *Front Oncol*. 2021;10:575317. doi:10.3389/FONC.2020.575317/PDF

40. Yersal O, Barutca S. Biological subtypes of breast cancer: Prognostic and therapeutic implications. *World J Clin Oncol*. 2014;5(3):412. doi:10.5306/WJCO.V5.I3.412

41. Łukasiewicz S, Czeczelewski M, Forma A, Baj J, Sitarz R, Stanisławek A. Breast Cancer—Epidemiology, Risk Factors, Classification, Prognostic Markers, and Current Treatment

Strategies—An Updated Review. *Cancers (Basel)*. 2021;13(17). doi:10.3390/CANCERS13174287

42. Gamble P, Jaroensri R, Wang H, et al. Determining breast cancer biomarker status and associated morphological features using deep learning. *Communications Medicine 2021 1:1*. 2021;1(1):1-12. doi:10.1038/s43856-021-00013-3

43. Mostafa IM, Tian Y, Anjum S, et al. Comprehensive review on the electrochemical biosensors of different breast cancer biomarkers. *Sens Actuators B Chem*. 2022;365:131944. doi:10.1016/J.SNB.2022.131944

44. Tarighati E, Keivan H, Mahani H. A review of prognostic and predictive biomarkers in breast cancer. *Clinical and Experimental Medicine 2021 23:1*. 2022;23(1):1-16. doi:10.1007/S10238-021-00781-1

45. Yadav R, Kumar Y, Dahiya D, Bhatia A. Claudins: The Newly Emerging Targets in Breast Cancer. *Clin Breast Cancer*. 2022;22(8):737-752. doi:https://doi.org/10.1016/j.clbc.2022.09.001

46. Baranwal S, Alahari SK. Molecular mechanisms controlling E-cadherin expression in breast cancer. *Biochem Biophys Res Commun*. 2009;384(1):6-11. doi:https://doi.org/10.1016/j.bbrc.2009.04.051

47. Corso G, Figueiredo J, De Angelis S Pietro, et al. E-cadherin deregulation in breast cancer. *J Cell Mol Med*. 2020;24(11):5930-5936. doi:10.1111/JCMM.15140

48. Feng Y, Spezia M, Huang S, et al. Breast cancer development and progression: Risk factors, cancer stem cells, signaling pathways, genomics, and molecular pathogenesis. *Genes Dis*. 2018;5(2):77-106. doi:10.1016/J.GENDIS.2018.05.001

49. Tay TKY, Tan PH. Liquid biopsy in breast cancer: A focused review. *Arch Pathol Lab Med*. 2021;145(6):678-686. doi:10.5858/arpa.2019-0559-RA

50. Alimirzaie S, Bagherzadeh M, Akbari MR. Liquid biopsy in breast cancer: A comprehensive review. *Clin Genet*. 2019;95(6):643-660. doi:10.1111/cge.13514

51. Aminolroayaei F, Shahbazi-Gahrouei D, Shahbazi-Gahrouei S, Rasouli N. Recent nanotheranostics applications for cancer therapy and diagnosis: A review. *IET Nanobiotechnol*. 2021;15(3):247. doi:10.1049/NBT2.12021

52. Benedet RDolores, Rounsaville MC. Understanding lumpectomy : a treatment guide for breast cancer. :159.

53. Bland KI, Klimberg VS. Master techniques in general surgery: Breast surgery. *Master Techniques in General Surgery: Breast Surgery*. Published online March 28, 2012:1-1152.

54. Loukas M, Tubbs RS, Mirzayan N, Shirak M, Steinberg A, Shoja MM. The history of mastectomy. *American Surgeon*. 2011;77(5):566-571. doi:10.1177/000313481107700515

55. Aggarwal V, Tuli HS, Varol A, et al. Role of reactive oxygen species in cancer progression: Molecular mechanisms and recent advancements. *Biomolecules*. 2019;9(11). doi:10.3390/biom9110735

56. Panieri E, Santoro MM. Ros homeostasis and metabolism: A dangerous liason in cancer cells. *Cell Death Dis*. 2016;7(6). doi:10.1038/cddis.2016.105

57. Wang Y, Qi H, Liu Y, et al. The double-edged roles of ROS in cancer prevention and therapy. *Theranostics*. 2021;11(10):4839-4857. doi:10.7150/thno.56747

58. Nakamura H, Takada K. Reactive oxygen species in cancer: Current findings and future directions. *Cancer Sci*. 2021;112(10):3945-3952. doi:10.1111/cas.15068

59. Liang W, He X, Bi J, Hu T, Sun Y. Role of reactive oxygen species in tumors based on the 'seed and soil' theory: A complex interaction (Review). *Oncol Rep*. 2021;46(3). doi:10.3892/or.2021.8159

60. Bhattacharyya A, Chattopadhyay R, Mitra S, Crowe SE. Essential Factor in the Pathogenesis of Gastrointestinal Mucosal Diseases. *Physiol Rev*. 2014;94:329-354. doi:10.1152/physrev.00040.2012.-Reactive

61. Phaniendra A, Jestadi DB, Periyasamy L. Free Radicals: Properties, Sources, Targets, and Their Implication in Various Diseases. *Indian Journal of Clinical Biochemistry*. 2015;30(1):11-26. doi:10.1007/s12291-014-0446-0

62. Arfin S, Jha NK, Jha SK, et al. Oxidative stress in cancer cell metabolism. *Antioxidants*. 2021;10(5). doi:10.3390/antiox10050642

63. Liberti M V., Locasale JW. The Warburg Effect: How Does it Benefit Cancer Cells? *Trends Biochem Sci*. 2016;41(3):211-218. doi:10.1016/j.tibs.2015.12.001

64. Liou GY, Storz P. Reactive oxygen species in cancer. *Free Radic Res*. 2010;44(5):479-496. doi:10.3109/10715761003667554

65. Wei C, Huang Q, Hu S, et al. Simultaneous electrochemical determination of hydroquinone, catechol and resorcinol at Nafion/multi-walled carbon nanotubes/carbon dots/multi-walled carbon nanotubes modified glassy carbon electrode. *Electrochim Acta*. 2014;149:237-244. doi:10.1016/J.ELECTACTA.2014.10.051

66. Qu Y, Han B, Yu Y, et al. Evaluation of MCF10A as a reliable model for normal human mammary epithelial cells. *PLoS One*. 2015;10(7):1-16. doi:10.1371/journal.pone.0131285

67. What is FTIR Spectroscopy? Accessed May 26, 2023. https://www.sigmaaldrich.com/PT/en/technical-documents/technical-article/analytical-chemistry/photometry-and-reflectometry/ftir-spectroscopy

68. IR Spectrum Table. Accessed March 16, 2023. https://www.sigmaaldrich.com/PT/en/technical-documents/technical-article/analytical-chemistry/photometry-and-reflectometry/ir-spectrum-table

69. Monzavi-Karbassi B, Hine RJ, Stanley JS, et al. Fructose as a carbon source induces an aggressive phenotype in MDA-MB-468 breast tumor cells. *Int J Oncol*. 2010;37(3):615. doi:10.3892/IJO_00000710

70. Woitassek D, Moya-Cancino JG, Sun Y, et al. Sweet, Sugar-Coated Hierarchical Platinum Nanostructures for Easy Support, Heterogenization and Separation. *Chemistry (Switzerland)*. 2022;4(4):1147-1160. doi:10.3390/CHEMISTRY4040078/S1

71. He H, Wang X, Feng Z, et al. Rapid microwave-assisted synthesis of ultra-bright fluorescent carbon dots for live cell staining, cell-specific targeting and in vivo imaging. *J Mater Chem B*. 2015;3(24):4786-4789. doi:10.1039/C5TB00570A

72. Yang X, Yang X, Li Z, et al. Photoluminescent carbon dots synthesized by microwave treatment for selective image of cancer cells. *J Colloid Interface Sci*. 2015;456:1-6. doi:10.1016/J.JCIS.2015.06.002

73. Wang L, Bi Y, Hou J, et al. Facile, green and clean one-step synthesis of carbon dots from wool: Application as a sensor for glyphosate detection based on the inner filter effect. *Talanta*. 2016;160:268-275. doi:10.1016/J.TALANTA.2016.07.020

74. Vale N, Silva S, Duarte D, Crista DMA, Pinto da Silva L, Esteves da Silva JCG. Normal breast epithelial MCF-10A cells to evaluate the safety of carbon dots. *RSC Med Chem*. 2021;12(2):245. doi:10.1039/D0MD00317D

75. Thompson EA, Graham E, Macneill CM, et al. Differential response of MCF7, MDA-MB-231, and MCF 10A cells to hyperthermia, silver nanoparticles and silver nanoparticle-induced photothermal therapy. *http://dx.doi.org/103109/026567362014936051*. 2014;30(5):312-323. doi:10.3109/02656736.2014.936051

76. Al Tamimi S, Ashraf S, Abdulrehman T, et al. Synthesis and analysis of silver–copper alloy nanoparticles of different ratios manifest anticancer activity in breast cancer cells. *Cancer Nanotechnol*. 2020;11(1):1-16. doi:10.1186/S12645-020-00069-1/FIGURES/6

77. Di Gregorio J, Petricca S, Iorio R, Toniato E, Flati V. Mitochondrial and metabolic alterations in cancer cells. *Eur J Cell Biol*. 2022;101(3). doi:10.1016/j.ejcb.2022.151225

78. Mellman I, Yarden Y. Endocytosis and cancer. *Cold Spring Harb Perspect Biol*. 2013;5(12). doi:10.1101/cshperspect.a016949

79. Havrdová M, Urbančič I, Bartoň Tománková K, Malina L, Štrancar J, Bourlinos AB. Self-targeting of carbon dots into the cell nucleus: Diverse mechanisms of toxicity in NIH/3T3 and l929 cells. *Int J Mol Sci*. 2021;22(11). doi:10.3390/ijms22115608

80. Ahmad MA, Aung YY, Widati AA, et al. A Perspective on Using Organic Molecules Composing Carbon Dots for Cancer Treatment. *Nanotheranostics*. 2023;7(2):187-201. doi:10.7150/ntno.80076

81. Lugano R, Ramachandran M, Dimberg A. Tumor angiogenesis: causes, consequences, challenges and opportunities. *Cellular and Molecular Life Sciences*. 2020;77(9):1745-1770. doi:10.1007/s00018-019-03351-7

82. Redza-Dutordoir M, Averill-Bates DA. Activation of apoptosis signalling pathways by reactive oxygen species. *Biochim Biophys Acta Mol Cell Res*. 2016;1863(12):2977-2992. doi:10.1016/j.bbamcr.2016.09.012

83. A Hileman E, Achanta G, Huang P. *Superoxide Dismutase: An Emerging Target for Cancer Therapeutics 698*.; 2001.

84. Griess B, Tom E, Domann F, Teoh-Fitzgerald M. Extracellular Superoxide Dismutase and its Role in Cancer. *Free Radic Biol Med*. 2017;112:464. doi:10.1016/J.FREERADBIOMED.2017.08.013

85. Guo CY, Sun L, Chen XP, Zhang DS. Oxidative stress, mitochondrial damage and neurodegenerative diseases. *Neural Regen Res*. 2013;8(21):2003. doi:10.3969/J.ISSN.1673-5374.2013.21.009